Article scientifique   Article   2025

Published version   Open Access

Plasticity of human resilience mechanisms

Leone, Giovanni; Casanave, Hannah; Postel, Charlotte; Fraisse, Florence; Vallée, Thomas; de La Sayette, Vincent; Dayan, Jacques; Peschanski, Denis; Eustache, Francis; Gagnepain, Pierre

COGNITIVE NEUROSCIENCE

Plasticity of human resilience mechanisms

Giovanni Leone[1,2,3], Hannah Casanave[1], Charlotte Postel[1], Florence Fraisse[1], Thomas Vallée[1],
Vincent de La Sayette[1], Jacques Dayan[1,4], Denis Peschanski[5],
Francis Eustache[1], Pierre Gagnepain[1]*

The hippocampus's vulnerability to trauma-induced stress can lead to pathophysiological disturbances that precipitate the development of posttraumatic stress disorder (PTSD). The mechanisms of resilience that foster remission and mitigate the adverse effects of stress remain unknown. We analyzed the evolution of hippocampal morphology between 2016/2017 and 2018/2019, as well as the memory control mechanisms crucial for trauma resilience. Participants were individuals exposed to the 2015 Paris terrorist attacks ($N = 100$), including chronic ($N = 34$) and remitted ($N = 19$) PTSD, and nonexposed ($N = 72$). We found that normalization of inhibitory control processes, which regulate the resurgence of intrusive memories in the hippocampus, not only predicted PTSD remission but also preceded a reduction in traumatic memories. Improvement in control mechanisms was associated with the interruption of stress-induced atrophy in a hippocampal region that includes the dentate gyrus. Human resilience to trauma is characterized by the plasticity of memory control circuits, which interacts with hippocampal neuroplasticity.

INTRODUCTION

Resilience is a fundamental aspect of human nature, reflecting the dynamic, plastic, and adaptive response of the brain to mitigate the damaging effects of stress. Maintenance or development of resilience mechanisms precedes recovery from trauma exposure (1–4). Resilience is not merely the opposite of vulnerability or a static trait but a dynamic process. However, neurobiological theories of posttraumatic stress disorder (PTSD) have primarily focused on stress vulnerability, leaving the neural mechanisms underlying resilience largely unexplored (5, 6).

Within this vulnerability framework, hippocampal alterations in both structure (7–10) and function (11, 12) play a key role in the formation of traumatic memories. These changes, along with interactions involving the amygdala and medial prefrontal cortex, can impair mechanisms of memory consolidation, extinction, and contextual processing (13–18). This can promote the encoding of fragmented, sensory, and emotional aspects of the traumatic event, often devoid of spatiotemporal context (19, 20). Such vulnerability of the memory system to stress (21) contributes to intrusive reexperiencing of trauma, a core feature of PTSD (22).

Hippocampal preexisting vulnerabilities (23–26) are implicated in PTSD development, while larger hippocampal volumes may act as a protective neural reserve (2) against stress (27). Posttraumatic longitudinal studies have so far revealed that the morphological alteration of the hippocampus (28, 29) or its subfields (30, 31) is stable with time, consistent with a predisposing factor. These findings challenge the long-standing theory that stress-induced hippocampal alterations explain the persistence of chronic PTSD (32). However,

this may reflect a lack of sensitivity of human brain morphological studies, especially with low-resolution magnetic resonance imaging (MRI), to the detrimental effects of stress on the hippocampal neuroarchitecture observed in animal models of PTSD (33). At the functional level, modulating hippocampal activity during memory processing is crucial for recovery and limiting the persistence of traumatic memory (17, 34–37).

In a previous study, we proposed that prefrontal inhibition of hippocampal activity during intrusive memory reexperiencing is critical for understanding resilience to trauma (38). This inhibition, linked to memory suppression, typically reduces memory vividness and intrusiveness (39–43). We examined individuals exposed and nonexposed to the 2015 Paris attacks, using the think/no-think (TNT) task while recording brain activity via functional MRI (fMRI). A year after the attacks, resilient individuals demonstrated preserved prefrontal down-regulation of intrusive memories in brain regions involved in trauma persistence, such as the hippocampus and precuneus. In contrast, those with PTSD exhibited compromised brain dynamics, failing to distinguish between intrusive and nonintrusive conditions.

In a follow-up study, we combined computational modeling with dynamic causal modeling of brain activity (44). We showed that individuals' beliefs about future intrusive experiences influence memory control processes. Specifically, control resources are shaped by prior experiences with suppression cues and the associated memories of particular items that predict future intrusions and trigger proactive avoidance strategies. Reactive control (RC), on the other hand, is engaged when intrusive memories bypass these proactive defenses, triggering a prediction error (PE) and additional inhibitory responses. In individuals with PTSD, the right middle frontal gyrus (rMFG) failed to properly down-regulate the hippocampus during reactive control. Instead, it showed excessive predictive control, mirroring maladaptive anticipatory strategies. In contrast, resilient individuals demonstrated an optimal balance between predictive control and reactive purging of intrusions during memory suppression (44).

These findings suggest that the effectiveness of memory control mechanisms is central to trauma resilience. However, because of the cross-sectional nature of our previous study, we could not establish a direct link between inhibitory control imbalance and resilience or

[1]Normandie Univ, UNICAEN, PSL Research University, EPHE, INSERM, U1077, CHU de Caen, GIP Cyceron, Neuropsychologie et Imagerie de la Mémoire Humaine, 14000 Caen, France. [2]Laboratory of Behavioural Neurology and Imaging of Cognition, Department of Neuroscience, Campus Biotech, University of Geneva, Geneva, Switzerland. [3]Swiss Center for Affective Sciences, University of Geneva, Geneva, Switzerland. [4]Pôle Hospitalo-Universitaire de Psychiatrie de l'Enfant et de l'Adolescent, Centre Hospitalier Guillaume Régnier, Université Rennes 1, 35700 Rennes, France. [5]Université Paris I Panthéon Sorbonne, HESAM Université, EHESS, CNRS, UMR8209, Paris, France.
*Corresponding author. Email: pierre.gagnepain@inserm.fr

PTSD recovery. PTSD persistence is closely linked to the distress caused by intrusive memories (*45*), implying that inhibitory control mechanisms are essential for resilience, not only for reducing memory vividness but also for mitigating stress's chronic effects on the brain associated with intrusive thinking. Prior research has shown a close connection between memory control and emotional regulation (*41, 46–48*). Memory suppression training has been shown to improve mental health during stressful life events (*49*). However, whether recovery from trauma is related to the plasticity of memory control mechanisms and whether such adaptation can protect the hippocampus from chronic stress remain unclear.

To investigate these questions, we conducted a longitudinal study (Fig. 1), collecting markers of hippocampal integrity and memory control mechanisms using the same TNT task and computational model as in our prior studies [see Materials and Methods and (*38, 44, 50*)]. Participants were individuals exposed to the 2015 Paris terrorist attacks. We collected fMRI, high-resolution (0.39 mm by 0.39 mm by 2 mm) MRI data focusing on the hippocampus, as well as an assessment of symptoms severity using a PTSD checklist version DSM-5 (PCL-5) (*51*), at two time points: 8 to 18 months after the event (time 1) and 30 to 42 months after (time 2). The sample included 72 nonexposed participants and 100 exposed participants. Clinical interviews based on DSM-5 criteria revealed that 34 exposed participants had chronic PTSD, 19 had remitted PTSD, 43 were asymptomatic at both time points, and 4 developed late-onset PTSD. These late-onset PTSD participants were excluded from further analyses, due to the small sample size. A clinical follow-up 5 years after the attacks (time 3) was also performed by a trained psychologist through a phone assessment of symptoms severity with

the PCL-5. Critically, this third phase of the study allowed us to assess whether changes in memory control and hippocampal markers of PTSD may precede and predict future evolution of symptoms.

We replicated the time 1 analysis (*44, 50*) for the time 2 data. We measured the volumes of hippocampal subfields using semiautomatic segmentation protocol of the high-resolution MRI images [see Materials and Methods and (*50*) for more details]. We focused this longitudinal analysis on two subfields whose alterations were mainly associated with PTSD, namely, the cornu ammonis 1 (CA1) and a mixture region composed of the dentate gyrus (DG), CA2, and CA3 subfields, given the unreliable separation between these subfields (*50, 52, 53*). We also examined fMRI activity during the memory suppression task (*54*), analyzing how top-down suppression of hippocampal activity changed over time and with clinical status. Participants learned a series of association pairs between words and pictures representing objects, which were counterbalanced between time points. Following this phase, participants then tried to stop the memory of the object from entering awareness (no-think) during the TNT phase, which also includes trials for which they had to recall the associated object (think). If the object comes to mind anyway during suppression attempts, then they are asked to push it out of mind and to report after the end of the trial that the reminder elicited an intrusion of its paired object (Fig. 2).

Building on our previous study at time 1, we used the same computational model of subjective intrusions to estimate the underlying beliefs about the probability of reexperiencing an intrusion and the related PE. We then evaluated the influence of these computational indexes on the top-down coupling from the middle frontal gyrus (MFG) to the hippocampus using a dynamic causal modeling
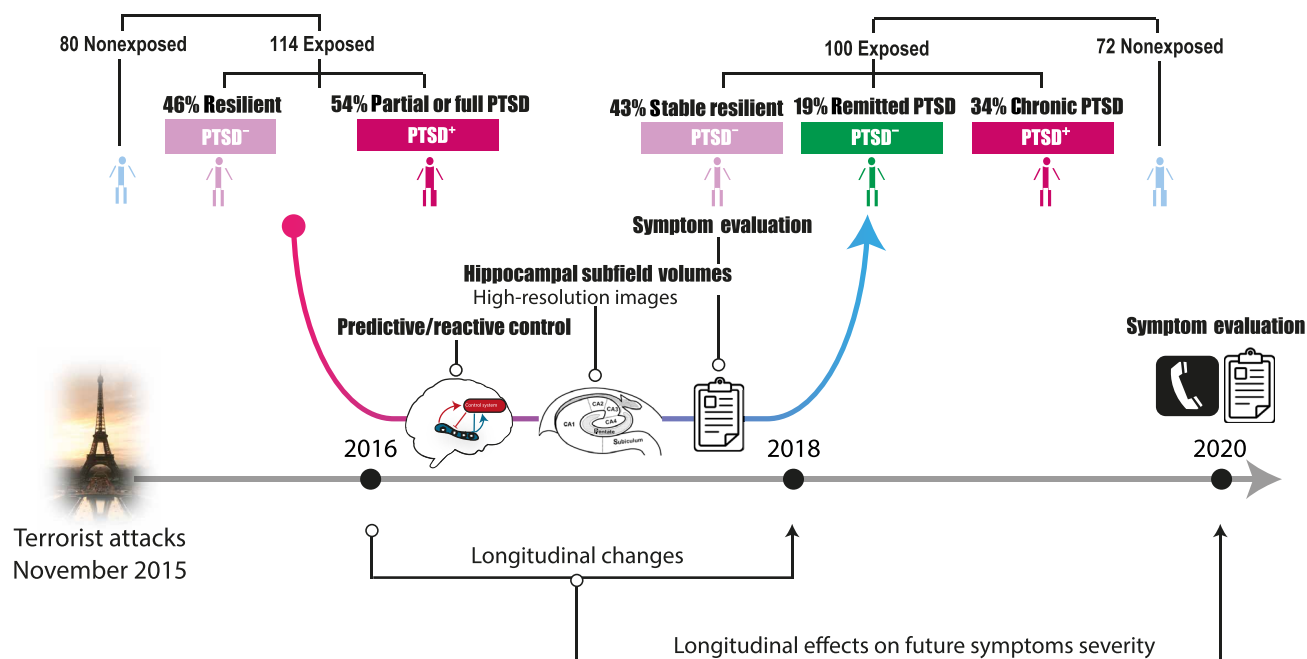

Fig. 1. Longitudinal design. Indexes of memory control and hippocampal integrity were collected at two time points after the 2015 Paris terrorist attack: 8 to 18 months (time 1) and 30 to 42 months (time 2). Participants with a similar degree of exposure were diagnosed in both time points as non-PTSD (PTSD⁻), chronic PTSD (PTSD⁺), or remitted PTSD (i.e., recovered from an initial PTSD at time 1). The intensity of PTSD symptoms was also measured in a third time point collected 5 years after the attacks. We analyzed longitudinal changes between time 1 and time 2 in the markers of interest: (i) the top-down regulation of hippocampal activity during intrusion control originating from the right DLPFC and (ii) the volumes of hippocampal subfields, including the CA1 and a mixture region composed of the close by DG, CA2, and CA3 subfields. We also investigated how those changes preceded the future evolution of symptoms using a third time point.
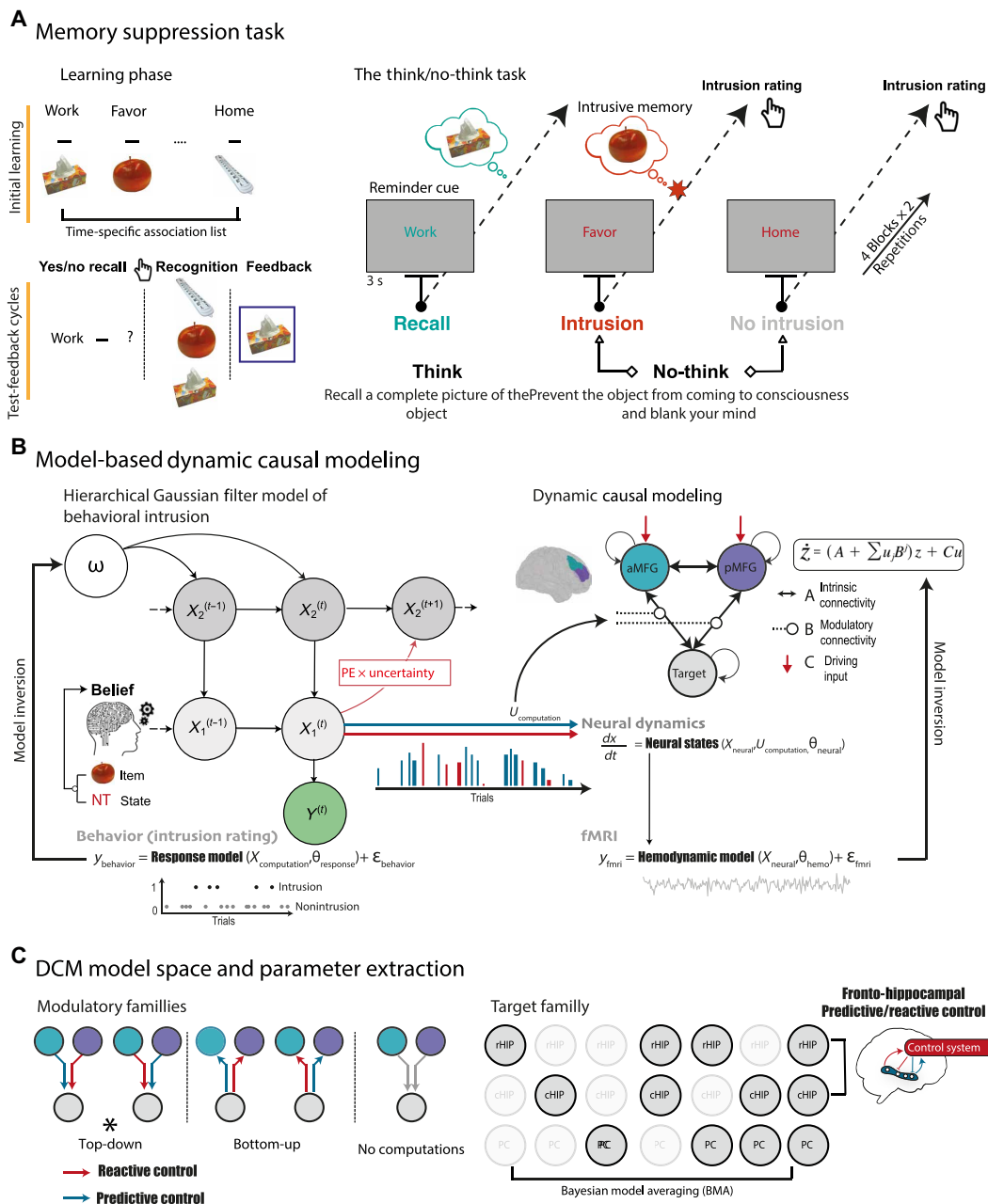
Fig. 2. Memory suppression task and model-based dynamic causal modeling (DCM). (**A**) Participants learned pairs of words and pictures of an object in a series of test-feedback cycles until they reached 90% of correct response. A new study list was proposed at each time point. Lists were counterbalanced between time points and conditions. Then, participants performed the TNT task in the MRI. For think items, participants recalled a detailed image of the associated object. For No-think items, participants had to prevent the picture from entering awareness and to remove it from consciousness if it came to mind. After each trial, participants reported the extent to which the associated image entered their awareness (intrusion). (**B**) Binary intrusion ratings were fed into a HGF (*116*) including two levels in which the dynamic updating of beliefs is weighted by uncertainty. The parameter ω regulates the speed of beliefs adjustment. Beliefs are assumed to arise from the precision-weighted combination of the memories about previous trials and specific word-object pairs. Beliefs and positive PEs were then used as parametric modulators of the top-down coupling between control and memory systems (B matrix). (**C**) DCM space expressing different hypotheses about computational influence on the modulation of the coupling between control regions [anterior and posterior middle frontal gyrus (aMFG and pMFG, respectively)] and memory target regions, including the rostral hippocampus (rHIP), caudal hippocampus (cHIP), and precuneus (PCu). Null models were also estimated but are not shown here. The computational model and the winning DCM family describing a top-down influence of computational indexes were identified at time 1 in (*44*). Here, we implemented Bayesian model averaging (BMA) in the family of models that won at time 1 and focused on fronto-hippocampal coupling previously associated with a control effect in PTSD.

(DCM) analysis, differentiating between predictive (i.e., intrusion belief) and reactive (PE) forms of memory control [see (44), Materials and Method, and Fig. 2 for more details on the computational model and DCM space].

We began by testing the hypothesis that remission from PTSD is accompanied by a plastic rebalancing of memory control mechanisms. According to this hypothesis, the imbalance observed at time 1 between predictive and reactive control should disappear at time 2 in individuals who have achieved remission (i.e., a Time*Control interaction). This improvement in control mechanisms should be specific to the remitted group and absent in other groups (i.e., a Time*Control*Group interaction). We also explored the temporal dynamics of the relationship between memory control and clinical improvement, hypothesizing that enhanced inhibitory control over unwanted memories between time 1 and time 2 would predict symptom reduction at time 3, reflecting a predictive marker of resilience. Next, we tested the hypothesis that prolonged PTSD at both time points would further impair hippocampal structure (time effect). This effect should be absent in individuals in remission, who may instead show plastic changes, such as increased hippocampal volumes, as well as in the other groups (i.e., a Time*Group interaction). Last, we examined whether improvements in memory control mechanisms were associated with a reduction in hippocampal atrophy, aligning with resilience models that propose that these mechanisms are engaged to mitigate the negative effects of stress on the brain.

RESULTS

Intrusion report during memory suppression

In healthy individuals, intrusion frequency decreases with repeated suppression of unwanted memory retrieval, reflecting a negative intrusion slope (39, 41, 55). Linear mixed effect (LME) analysis, including group and time as fixed effects, revealed that the slope of intrusion control was significantly negative in nonexposed [$T = -9.69$,

$P < 0.0001$, 95% confidence interval (CI) = [−1.06 to 0.70], df = 156.96], PTSD⁻ ($T = -5.51$, $P < 0.0001$, 95% CI = [−0.89 to 0.42], df = 156.96), remitted PTSD ($T = -2.88$, $P = 0.004$, 95% CI = [−0.88 to 0.16], df = 156.88), and PTSD⁺ ($T = -6.28$, $P < 0.0001$, 95% CI = [−1.10 to 0.57], df = 151.63) groups. The slope of intrusion control did not differ between time points for each of these groups (all P values > 0.15), and no Group*Time interactions were observed (all P values > 0.17).

Remission of PTSD is associated with the adaptive plasticity of memory control processes

Analysis of intrusion behavioral reports indicated that individuals exposed to trauma, even after developing PTSD, can still exert control over neutral intrusive memories during the memory suppression task. In a previous study, we found that the preservation of such capacities relies on the aberrant and excessive engagement of predictive control in individuals with PTSD, while reactive control is altered, provoking a substantial imbalance between both forms of control (44). Such control imbalance was absent in resilient and nonexposed participants, who showed a similar and balanced level of inhibitory coupling between both forms of control. Here, we used a single LME model, fitting all groups and time points at once, to study the longitudinal changes on top-down coupling parameters associated with predictive and reactive control (see Materials and Methods).

Control*Time interaction

We first tested whether memory control imbalance disappeared in participants who remitted from PTSD at time 2. A Control*Time interaction in the remitted group revealed the association between remission of PTSD and the recovery between time points of a balanced control process [$T = 2.31$, P false discovery rate (P-fdr) = 0.045, 90% CI = [0.19 to 1.14], df = 157.2; Fig. 3]. Further planned comparisons performed within this interaction showed that, although remitted PTSD showed a significant imbalance at time 1 (control
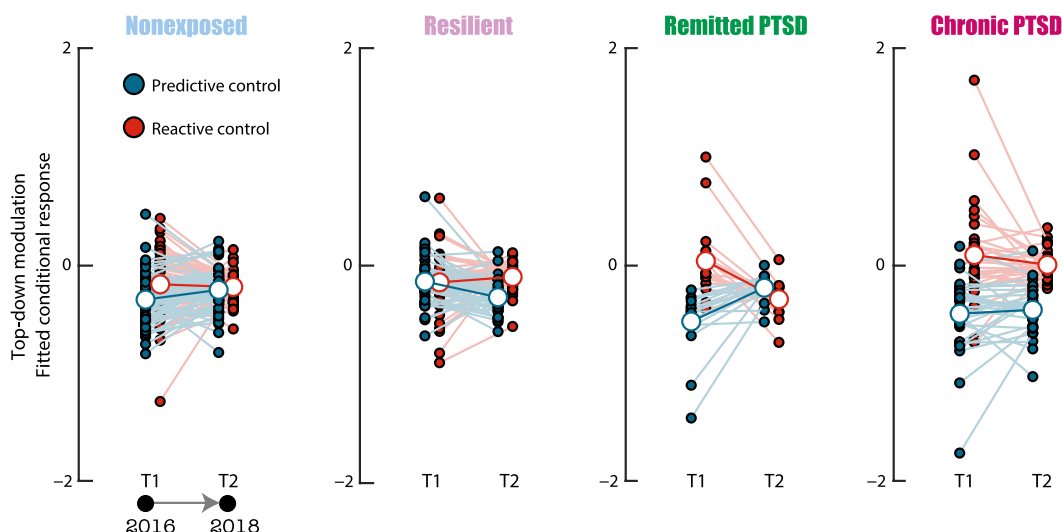

Fig. 3. Remission from PTSD is associated with the plastic restoration of the balance between predictive and reactive memory control. Small blue and red circles represent the modulation of the top-down coupling from the MFG to the hippocampus during predictive control and reactive control, respectively, at time 1 and time 2, for each individual (as predicted by the LME, i.e., fitted conditional response). Larger dots and bold lines represent the fixed effects of control and time at the group level. Remitted PTSD was characterized by a gain balance between predictive control and reactive control at time 2, while no significant evolution was observed in the other groups.

effect: $T = 2.301$, P-fdr = 0.023, 90% CI = [0.16 to 0.96], df = 152.32), the recovery of control mechanisms in this group was driven by an improvement of reactive control (time effect: $T = 1.812$, P-fdr = 0.044, 90% CI = [0.03 to 0.68]) and reduction of predictive control (time effect: $T = -1.72$, P-fdr = 0.044, 90% CI = [−0.61 to −0.011]). Moreover, RC was now characterized by a negative coupling parameter at time 2 in this group ($T = -2.57$, P-fdr = 0.024, 90% CI = [−0.52 to −0.11]). Chronic PTSD underwent no significant evolution with time, as shown by the absence of significant Control*Time interaction in this group ($T = 0.59$, P-fdr = 0.28, 90% CI = [−0.12 to 0.35], df = 159.8). Further planned comparisons revealed that chronic PTSD was characterized by a significant difference between predictive control and reactive control at time 1 ($T = 3.019$, P-fdr = 0.001, 90% CI = [0.25 to 0.84], df = 152.4) and at Time 2 ($T = 3.08$, P-fdr = 0.001, 90% CI = [0.19 to 0.64], df = 159.06). Moreover, we confirmed that the balance between both forms of control previously observed (*44*) was stable in time in both resilient (Control*Time interaction: $T = -1.03$, P-fdr = 0.28, 90% CI = [−0.51 to 0.12], df = 158.7) and nonexposed participants (Control*Time interaction: $T = 0.791$, P-fdr = 0.28, 90% CI = [−0.12 to 0.35], df = 158.3).

Group*Control*Time interaction
To further confirm the normalization of inhibitory control processes at time 2 in individuals who are remitted from PTSD, we compared the Control*Time interaction that we previously observed in this group to the interaction pattern in the other groups (characterized by a temporal stability of control processes). This analysis revealed that the decrease of memory control imbalance through time in the remitted group was significantly different from the temporal profile of the other groups (Control*Group*Time interaction: $T = 2.11$, $P = 0.018$, 90% CI = [0.14 to 1.16], df = 157.8). At time 2, the difference between reactive control and predictive control processes in remitted PTSD was no longer different from the pattern observed in nonexposed (Control*Group interaction at time 2: $T = -0.63$, P-fdr = 0.26, 90% CI = [−0.48 to 0.21], df = 159.1) or resilient (Control*Group interaction at time 2: $T = -1.14$, P-fdr = 0.14, 90% CI = [−0.66 to 0.07], df = 159.1) but became significantly different compared with the persistent imbalance observed in chronic PTSD (Group*Control interaction at time 2: $T = -2.28$, P-fdr = 0.036, 90% CI = [−0.90 to −0.14], df = 159.1).

Imbalance analysis
To confirm the reduction of the imbalance between predictive control and reactive control with the remission of PTSD, we computed the index of imbalance between these two forms of control (*44*). In this framework, predictive control and reactive control are conceptualized as two independent yet downward forces, jointly mitigating hippocampal activity and serving the same downregulation function of memory processes (see Materials and Methods). The imbalance is reflected in the direction of the resultant vector combining these two orthogonal forces, with an imbalance in favor of either predictive control (from 0° to 180°, moving anticlockwise) or reactive control (from 0° to −180°, moving clockwise). Parametric two-way analysis of variance (ANOVA) for circular data confirmed the presence of a significant interaction ($P = 0.007$), between time and group (i.e., remitted versus chronic PTSD). This interaction was characterized by an absence of imbalance difference between both groups at time 1, while, at time 2, we observed that the imbalance decreased significantly in favor of

reactive control for individuals in remission compared with chronic PTSD ($F_{2,51} = 5.67$, $P = 0.021$).

Overall, these results suggest that the remission from PTSD 3 years after the trauma is associated with the plastic recovery of the top-down control mechanisms between the rMFG and the hippocampus, supporting the efficient suppression of intrusive memories. Like trauma-exposed participants without PTSD and nonexposed individuals, individuals in remission at time 2 are now able to optimally balance predictive control and reactive control during the memory suppression task. Conversely, exposed individuals with chronic PTSD continue to excessively use beliefs to control hippocampal activity during the task and fail to regulate unwanted intrusions with reactive mechanisms.

Adaptive plasticity of memory control forecasts reduction of traumatic memories
However, these results are not informative of the temporal dependencies between the recovery of memory control mechanisms and the reduction of the two cardinal features of traumatic memory, avoidance and traumatic reexperiencing, which we previously linked to control imbalance (*44*). On the one hand, the reduction of the maladaptive stress response associated with the general reduction in trauma severity could lead to the recovery of control mechanisms by improving prefrontal control functioning (*56*), highlighting a benefit of PTSD remission. On the other hand, plasticity of control mechanisms could precede a reduction of the traumatic memory, suggesting a causal relationship. Understanding the temporal dynamics of control mechanisms and symptoms' evolutions is fundamental to unveiling the nature of their relationship.

Capitalizing on interindividual variations in the modulation of control imbalance across time points in the group of participants suffering from chronic PTSD, we therefore tested the hypothesis that the apparition of remediated control mechanisms at time 2 might usher in a positive clinical evolution at time 3 (Fig. 4). To examine this question, we fit an LME model with the severity of PTSD symptoms at time 2 and time 3 as dependent variables and the longitudinal changes between time 1 and time 2 in the top-down imbalance of the reactive/predictive coupling parameters as independent variables (i.e., within-subject effect orthogonalized with respect to mean imbalance in coupling; see Materials and Methods) (*57*). Cross-sectional effects associated with interindividual variations in mean coupling parameters were also included in the model to separate between-subject effects from within-subject effects. Crucially, we found in individuals with chronic PTSD at time 2 a positive significant relationship between the temporal evolution of control imbalance and future changes in intrusive reexperiencing ($\beta = 1.08$, $T = 2.42$, P-fdr = 0.033, 90% CI = [0.28 to 1.88], df = 11.51]; Fig. 4). Regarding avoidance, a marginal relationship was observed ($\beta = 0.39$, $T = 1.59$, P-fdr = 0.069, 90% CI = [−0.047 to 0.82], df = 11.93]; Fig. 4). This positive relation indicates that the improvement of imbalance toward reactive control mechanisms between time 1 and time 2 precedes a reduction of intrusion severity between time 2 and time 3, while its degradation precedes a worsening of their severity. Critically, however, additional analyses revealed that this positive relationship was not observed for clusters of symptoms that cut across diagnostics boundaries (see the Supplementary Text). Together, these results demonstrate the major role of the memory control mechanisms to the persistence of traumatic memory in PTSD and highlight how
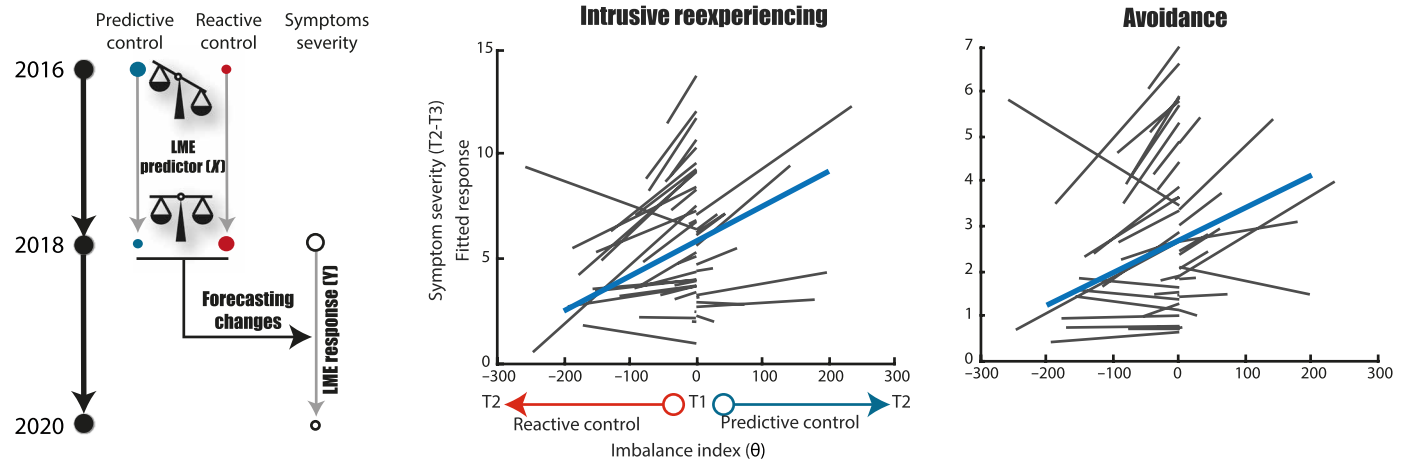
Fig. 4. Control plasticity forecasts traumatic memory evolution. The left panel shows the LME predictors and response for the forecasting analysis. On middle and right panels, the *x* axes show the evolution of the control index reflecting the balance between predictive control and reactive control at time 2 relative to time 1, expressed in degrees (see Materials and Methods). Across time points, the balance index can either evolve toward a gain in reactive control (left part of the plots, negative shift from T1) or toward a gain in predictive control (right part of the plots, positive shift from T1). We display the difference in imbalance between T1 and T2 for visualization purposes. On the *y* axes, symptoms' severity, predicted by the LME model (i.e., conditional response). Gray lines represent individual data points for each chronic PTSD participant, while the blue line represents the fixed effect at the population level. Improvement of reactive control forecasted the future reductions in intrusive reexperiencing (left) or avoidance (right) symptoms severity, while increase in predictive control had the opposite effect.

the neurocognitive plasticity of these mechanisms may prelude the remission of PTSD.

Chronic PTSD is associated with atrophy of CA2-3/DG

We then analyzed the effects of groups, time and subfield, on hippocampal volumes using LME. Age, sex, and total intracranial volume (TIV) were added as covariates to reduce unexplained variance. In the previous study conducted at time 1 in the same participants, we found smaller volumes for both CA1 and CA2-3/DG in individuals with PTSD compared to those in nonexposed and resilient individuals (*50*).

Time effect

A significant reduction of hippocampal volume with time was observed in chronic PTSD (time effect: $T = 2.034$, $P = 0.021$, 90% CI = [6.3 to 60.6], df = 275.33; Fig. 5). This main effect of time, however, did not survive correction for multiple comparisons across groups (P-fdr = 0.086). Considering the subfields separately, we observed in this group a significant reduction with time of the volume of CA2-3/DG (time effect: $T = 2.34$, P-fdr = 0.041, 90% CI = [7.5 to 43.8], df = 127.41). Although this effect was absent for CA1 (time effect: $T = 0.66$, P-fdr = 0.36, 90% CI = [−11.8 to 27.4], df = 127.95), no Time*Subfield interaction was observed in chronic PTSD ($T = 1.13$, $P = 0.13$, 90% CI = [−8.2 to 43.9], df = 232.28). Remitted individuals, however, did not undergo any significant volume change with time in the CA2-3/DG (time effect: $T = −1.039$, P-fdr = 0.21, 90% CI = [−38.8 to 8.9], df = 120.49) or CA1 (time effect: $T = 0.37$, P-fdr = 0.36, 90% CI = [−20.1 to 31.5], df = 122.36). Moreover, the volume of CA2-3/DG or CA1 did not change with time in resilient or nonexposed individuals (all P-fdr values > 0.15). However, the effect of time did not differ between CA2-3/DG and CA1, for any of the groups considered (all P-fdr values > 0.31).

Time*Group interaction

We then tested whether the longitudinal reduction of the volume of CA2-3/DG that we observed in chronic PTSD was significantly different to the longitudinal patterns of other groups, for which no further changes in time were observed. This test showed the presence of a significant Time*Group interaction ($T = 2.79$, $P = 0.003$, 90% CI = [14.2 to 55.6], df = 115.49), revealing that the progression of CA2-3/DG alteration is specific to chronic PTSD. However, although such an interaction was absent for CA1 ($T = 0.72$, $P = 0.23$, 95% CI = [−12.6 to 32.2], df = 117.77), no Time*Group*Subfield interaction was observed when Chronic PTSD was compared to other groups ($T = 1.36$, $P = 0.087$, 95% CI = [−5.3 to 55.5], df = 232.12).

These findings suggest that the chronification of stress in persistent PTSD can have a detrimental effect on the integrity of the CA2-3/DG. This finding is in line with evidence from animal studies showing that chronic stress impairs hippocampal morphology (*58*) and neurogenesis in the dentate gyrus (*59*, *60*), eventually leading to its atrophy. Yet, it remains unknown whether the observed pathophysiological process is specific to processes depending solely on this region given that no interaction with CA1 was observed.

We then analyzed the effects of longitudinal changes of CA2-3/DG volumes on the future evolution of symptoms between time 2 and time 3, as previously done with control mechanisms. We found no predictive effects of volume change on symptoms' severity (all P values > 0.26).

Memory control plasticity is linked to hippocampal morphological changes

Our findings show that adaptive plasticity in control mechanisms is linked with the remission of PTSD and further forecast a reduction in the persistence of the trauma. Moreover, an interruption of stress-induced alterations within the CA2-3/DG is observed in individual remitting from PTSD, while the chronification of this disorder is associated with atrophic changes in the volume of CA2-3/DG. We next sought to examine whether the evolution across time of the imbalance in memory control mechanisms was related to the changes
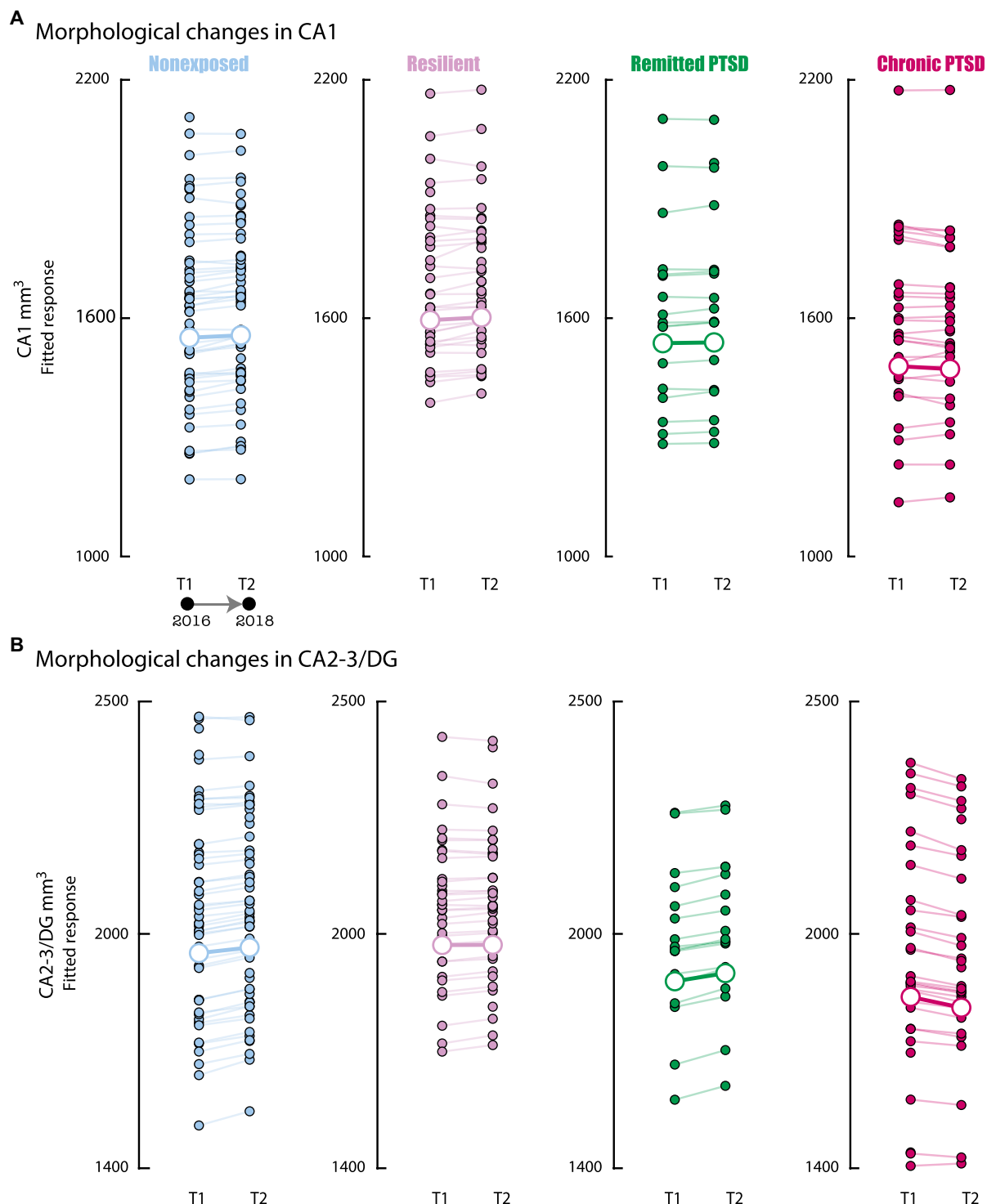
Fig. 5. Chronic PTSD is associated with atrophy of CA2-3/DG. Evolution of hippocampal subfields' volumes of CA1 (**A**) and CA2-3/DG (**B**) with time in nonexposed, resilient, remitted, and chronic PTSD groups (the *y* axes reflect the fitted conditional response of the LME model). Small dots and pale lines indicate individual data points. Larger dots and bold lines reflect the fixed effect of time at the group level. No morphological changes were observed in CA1 in any of the four groups. Chronic PTSD was associated with the atrophic reduction of CA2-3/DG volumes at time 2 compared to those at time 1, while no significant variations were observed in the other three groups.

observed in the volumes of the CA2-3/DG. To examine this question, we fit an LME model with the volume of the CA2-3/DG at time 1 and time 2 as a dependent variables and the longitudinal changes between time 1 and time 2 in the top-down imbalance of the reactive/predictive coupling parameters as an independent variables (together with the between-subject effect in mean imbalance). This analysis focuses on the relationship between slope of changes that occur in control mechanisms (improvement or degradation) and the temporal evolution of the hippocampus that occurs within individuals. In individuals that were initially diagnosed with PTSD at time 1, results revealed a negative relationship between the temporal evolution of control imbalance and volume of the CA2-3/DG ($\beta = -8.09$, $T = -1.73$, $P = 0.05$, 90% CI = [−16.2 to 0.00], df = 19.79). This negative relation indicates that, when individuals tend to improve memory control balance toward reactive mode, plastic increases in CA2-3/DG volumes tend to occur in parallel. On the other hand, when the memory control balance shifts toward predictive mode, CA2-3/DG volumes tend to decrease with time. In exposed participants, results revealed a similar negative relationship between the temporal evolution of control imbalance and volume of the CA2-3/DG ($\beta = -9.3$, $T = -2.37$, $P = 0.012$, 90% CI = [−16.9 to −2.8], df = 30.22; Fig. 6). However, this relationship disappeared when nonexposed individuals were analyzed instead ($\beta = -0.22$,

$T = -0.03$, $P = 0.49$, 90% CI = [−12.1 to 11.7], df = 6.55; Fig. 6), suggesting that the relationship between the plasticity of control and hippocampal mechanisms characterizes an important adaptive property of these circuits in response to trauma.

DISCUSSION
The primary objective of this longitudinal study was to investigate whether inhibitory control processes, dependent on the prefrontal cortex and potentially implicated in intrusive reexperiencing following trauma, improve over time and contribute to recovery from PTSD. Using a simple Bayesian computational model of intrusive reexperiencing during a memory suppression task, which captures the combined effects of predictive control and reactive control on fronto-hippocampal down-regulation, we found that a 2-year remission from PTSD is associated with a plastic rebalancing of memory control mechanisms. In contrast, no such changes were observed in individuals with chronic PTSD or those who were already resilient at the first time point. In individuals with PTSD, the excessive influence of predictions about future memory control demands (linked to intrusions) on fronto-hippocampal coupling during memory suppression diminished after remission. This reduction was paralleled by an improvement in the reactive purging of ongoing
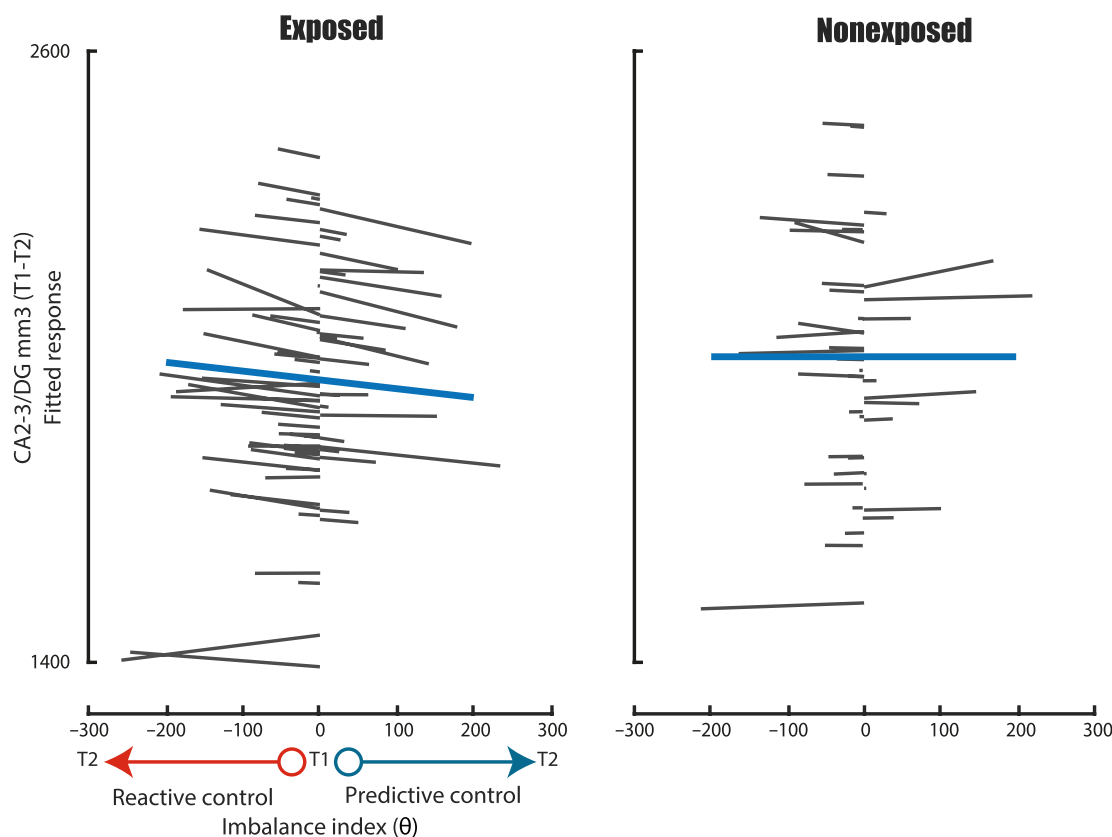
Fig. 6. Relationship between control plasticity and morphological changes in the hippocampus. On the x axes, the evolution of the control index, reflecting the balance between predictive control and reactive control at time 2 relative to that at time 1, expressed in degrees (see Materials and Methods). Across time points, the balance index can either evolve toward a gain in reactive control (left part of the plots) or toward a gain in predictive control (right part of the plots). On the y axes, CA2-3/DG volumes, predicted by the LME model (i.e., conditional response). Gray lines represent individual data points for each exposed (left) or nonexposed (right) participant, while the blue line represents the fixed effect at the population level. Improvement of reactive control in exposed individuals predicted parallel CA2-3/DG volumetric plastic changes, while no significant relationship was observed in nonexposed individuals.

intrusions, which became more effective. Tracking symptom changes over three time points (i.e., intrusive reexperiencing and avoidance) revealed that improvements in inhibitory control over unwanted memories between the first and second time points predicted positive outcomes at the third, highlighting a potential predictive marker of resilience. The study's second aim was to test whether chronic stress in individuals with PTSD further compromises the integrity of hippocampal structures, using high-resolution MRI scans of hippocampal subfields. While no changes in hippocampal subfield volume were observed in individuals who had remitted from PTSD or those without PTSD at the first time point, results indicated atrophy in the CA2-3/DG region in individuals with chronic PTSD. Last, in the trauma-exposed group and those diagnosed with PTSD at the first time point, our findings showed that the intraindividual slopes characterizing the temporal evolution of control mechanisms and hippocampal integrity were interrelated.

Current models of PTSD link the persistence of traumatic memory to preexisting vulnerabilities together with stress-induced alterations in fear and memory circuits (61). Complementary hypotheses suggest that PTSD is also characterized by deficits in inhibitory control circuits, which regulate activity in memory-processing areas and limit access to unwanted memories (38, 44). Our findings indicate that plastic resilience processes rooted in the memory control brain network can foster clinical improvement by protecting against the chronic deterioration of the hippocampus, aligning with models that suggest resilience mechanisms adaptively mitigate the negative effects of stress on the brain (1–4). These results bridge the gap between two distinct neurobiological frameworks in the literature that characterize variations in response to trauma, highlighting a fundamental mechanism of human brain resilience against trauma.

Many animal studies have documented the detrimental effects of chronic stress on the hippocampus, altering synaptic plasticity, dendritic morphology, neurogenesis, and neurodegeneration (62–67). However, these effects are not consistently replicated in human studies (30, 31, 66). Here, although the observed pattern is compatible with the idea that smaller hippocampal volumes reflect a preexisting vulnerability to PTSD (24, 27), we further observed the presence of atrophic changes in the CA2-3/DG region in individuals suffering from chronic PSTD. The novelty of our findings might be explained by the fact that other relevant studies used shorter clinical follow-ups and/or lower-resolution MRI sequences (24, 28, 30, 31). Furthermore, it is often challenging to include groups of individuals matched for the nature, onset, and duration of traumatic exposure, as was achieved here. These variations may limit the characterization of hippocampal alterations in PTSD. In line with our findings, animal studies show that chronic stress provokes a loss of dendritic complexity in the CA3, reducing synaptic connections (58, 68). Adult neurogenesis in the DG is also highly sensitive to stress (67, 69–71) and its interruption might exacerbate the progression of hippocampal atrophy. However, we did not observe the presence of a significant interaction between time and subfield in chronic PTSD, suggesting that the observed patterns of atrophic changes may not solely depend on pathophysiological processes specific to the DG (e.g., neurogenesis).

This study does not provide insight into the origin of resilience mechanisms or the precise temporal sequence of events, due to the sparsity of longitudinal measurements. Nevertheless, it offers valuable information on the role of inhibitory control mechanisms in the memory domain and their plasticity in recovery and adaptation

processes. Several elements suggest that the plasticity of memory inhibition processes may not only accompany and anticipate trauma remission but also limit stress-induced damage to the hippocampus, rather than the reverse. We observed positive changes in control processes associated with remission but not in hippocampal volumes, which showed no change in the remitted group but atrophic changes in chronic PTSD. These improvements in control processes predicted the reduction of intrusive reexperiencing, a core symptom of PTSD, and were associated with the interruption of hippocampal atrophy. Together, these findings suggest that the restoration of control mechanisms initiates remission, which may benefit the hippocampus and support the recovery process in a virtuous cycle.

Although it remains largely unknown whether this relationship depends on the restored capacity of the inhibitory control system to limit or modulate the traumatic reexperiencing itself, several arguments might suggest a potential connection. First, memory suppression not only silences unwanted memories or reduces their vividness but also regulates the negative emotions associated with those memories (46). Suppressing intrusive memories disrupts the emotional content of the suppressed traces (41), and stopping unwanted retrieval is associated with the parallel extinction of the related emotional responses (72). Frontal networks involved in memory and emotional control overlap (46, 48), and prefrontal control during emotional actions predicts resilience against PTSD (73). Intrusive memories in PTSD are often accompanied by intense and uncontrollable negative emotions, such as fear and sadness, profound distress, and the sensation that the traumatic event is happening again (74–76). The persistent reexperiencing of the traumatic experience characterizing chronic PTSD is accompanied by elevated systemic levels of oxidative stress and inflammation, due to sustained activation of the hypothalamic-pituitary-adrenal axis (77, 78). This maladaptive stress response can provoke a constant state of alert, hyperarousal, and altered fear response (79), further exacerbating intrusive memories in a maladaptive loop (80, 81). By limiting the access of the consciousness and attention to intrusive memories (55), the memory control system may break this negative cycle, reducing hippocampal damage caused by intrusion-related stress and their associated negative emotions.

Second, the rehabilitation of inhibitory control mechanisms could limit hippocampal hyperexcitability potentially associated with intrusive reexperiencing. Chronic stress increases glutamatergic signaling from amygdalar projections to the hippocampus (82, 83), selectively damaging GABAergic interneurons (84, 85) and disrupting the excitation/inhibition balance, resulting in hippocampal chronic hyperexcitability. This imbalance is central to many psychiatric disorders (86, 87) including PTSD (88). Although the relationship between intrusive memories and hippocampal hyperexcitability is still poorly understood (4, 89–91), down-regulation of intrusive memories in the hippocampus could help reduce such hyperexcitability via indirect prefrontal connection that activate GABAergic interneurons (92, 93), thereby mitigating the structural damage caused by hyperexcitability. In line with this perspective, stimulating the activity of hippocampal GABAergic transmission can lead to morphological and functional synaptic changes, as well as the formation of new inhibitory synapses (94). Furthermore, enhancing inhibition of stress-responsive DG neurons increases resilience to stress (95).

Third, such protecting effect of intrusion control on the DG may help restore neurogenesis-related and hippocampal functions, such

as pattern separation and contextual processing, further fostering resilience and adaptation to stress in a virtuous loop, as suggested for a long time by animal researchers (*67*, *69–71*). However, the lack of interaction between CA1 and CA2-3/DG and the absence of clear separation between CA2-3/DG in the current images leave uncertainty about whether the observed effects depend exclusively on DG-related physiological mechanisms, such as neurogenesis. For example, the restoration of GABAergic function in the hippocampus could relieve prefrontal function. Although we cannot disentangle the causal relationships between these phenomena, our findings suggest that recovery of memory control is linked to a cascade of morphological changes in the hippocampus, creating a virtuous loop that promotes resilience and recovery.

Limitations
This study has several limitations. Our computational model accounts for a limited range of cognitive mechanisms, while the control of intrusive memories in daily life involves a much more complex set of cognitive functions and processes (*96*). The model's formation of beliefs driving intrusion control reflects the memory of past trials and items, which likely depends on episodic memory. However, beyond this episodic guidance, adaptive top-down control is also influenced by other contextual or semantic information not modeled here (*97*). Overgeneralization of fear to new contexts may trigger intrusive reexperiencing (*13*), raising question about how contextually derived predictions may influence control. Maladaptive conceptual representations about context, such as the belief that the world is inherently dangerous, also constitute aberrant hyperpriors reinforcing avoidant behavior, contributing to the maintenance of intrusions (*98*). Furthermore, bottom-up sensory priors influence predictive processing (*99*), and traumatic experiences may bias perceptual and interoceptive hypotheses, triggering intrusive reexperiencing (*100*). Our experimental design and computational models do not account for these possibilities, leaving it unclear how such beliefs influence inhibitory control. Another limitation is that our model only captures intrusive memories at the behavioral level, not the neural dynamics underlying belief and PE updating, so it should not be viewed as a model of predictive coding. Despite these limitations, our results reveal that the plasticity of intrusion control mechanisms, dependent on memory-based predictive processing, is central to understanding resilience after trauma.

Another concern of this study is the limited sample size. In studies with smaller samples, the ability to detect a true effect of a certain magnitude is reduced. Due to the small size of the remitted group, we cannot rule out the possibility of smaller effects that we were unable to detect regarding hippocampal subfield plasticity following PTSD remission. Small samples also tend to produce parameter estimates and confidence intervals that are broad and imprecise. Therefore, the extent of changes associated with PTSD chronification or remission remains uncertain in this study, and replication with larger samples is necessary to provide more accurate estimates. This limitation is important for understanding the scope of potential clinical applications stemming from our findings. Additionally, the small sample size may hinder the identification of transdiagnostic mechanisms related to PTSD comorbidities, although we accounted for the influence of comorbidities, such as depression, as the cause of the observed pattern (see the Supplementary Text). PTSD is a heterogeneous disorder involving various neurocircuits, and small samples may limit the characterization of these circuits. Future studies with larger samples may provide more detailed insights into the generalization of the neurobiological substrate of intrusive thoughts. Our results should be interpreted in light of this limitation. However, note that the small size of the remitted group does not affect the reliability of our significant findings.

Concluding remarks
Consistent with the current understanding of resilience (*1–4*), the plasticity of inhibitory control mechanisms involved in memory suppression reflects a positive and dynamic adaptation after exposure to trauma, helping individuals overcome the stressful experience (*49*, *101*). This demonstrates that, although resilience depends on preexisting factors, such as prefrontal regulatory mechanisms (*73*), adaptive mechanisms can also be plastic and acquired. However, linking dynamic adaptation to inhibitory control mechanisms and frontal activity has not always succeeded when using motor inhibition tasks (*4*). While there are significant overlaps between neurocircuits involved in memory and motor control (*102*), the discrepancy suggests that dynamic resilience processes might be more effectively captured through fronto-hippocampal inhibitory coupling mechanisms and neurocognitive functions more closely related to PTSD symptoms, rather than motor inhibition tasks.

It remains unclear whether the remission of inhibitory control mechanisms identified in this study can disrupt the traumatic memory itself and complement existing trauma-focused exposure therapies. On one hand, if the traumatic memory is consolidated outside of the hippocampus and its reactivation is too strong, then attempts to suppress its retrieval may prove ineffective. Inadequate suppression attempts can also exacerbate emotional responses or the recurrence of intrusive memories (*41*, *47*, *55*). On the other hand, the independence of traumatic memory traces and intrusive reexperiencing from the hippocampus remains an open question (*4*, *89–91*), and the fronto-hippocampal pathway identified in this study may have contributed to the reduction of trauma. Limiting memory intrusiveness to a moderate level of activation and stimulating the inhibitory control system during trauma-focused treatments could facilitate the destabilization and forgetting of traumatic memories during reconsolidation (*103*, *104*). Similarly, practicing memory retrieval suppression may enhance extinction learning (*72*). Alternatively, activating prefrontal-inhibitory pathways during treatment could stimulate inhibitory plasticity, which would further promote the silencing of memory traces (*105*, *106*).

Despite these uncertainties, our findings indicate that the plasticity of inhibitory control circuits plays a crucial role in the positive adaptation to trauma and is more closely tied to hippocampal neuroplasticity under stress than previously recognized. These findings pave the way for new control-based treatments aimed at fostering resilience.

MATERIALS AND METHODS
Participants
Eighty nonexposed and 114 exposed subjects participated in this study (*38*). Exposed participants were recruited through the transdisciplinary and longitudinal research "Program 13-Novembre" (www.memoire13novembre.fr/), a nationwide funded program supported by victims' associations. Nonexposed participants were not present in Paris on 13 November 2015 and were recruited from a local panel of volunteers. A clinical interview with a medical doctor was conducted to ensure that participants had no reported history

of neurological, medical, visual, memory, or psychiatric disorders. Exclusion criteria also included history of alcohol or substance abuse (other than nicotine), mental or physical conditions that preclude MRI scanning (e.g., claustrophobia or metal implants), and medical treatment that may affect the central nervous system or cognitive functions. All the participants were between the ages of 18 and 60 years old, right-handed, and French speaking and had a body mass index inferior to 35 kg/m^2.

At both time points, exposed participants were diagnosed using the structured clinical interview of the DSM-5 (SCID) (107) conducted by a trained psychologist and supervised by a psychiatrist. To ensure that the SCID covers all relevant aspects of the PTSD it aims to diagnose, the interview was highly standardized, following a structured format that guided the clinicians through specific questions and criteria. This standardization ensured consistency in administration across participants. To further increase consistency in interpretations and the reliability of the diagnosis of PTSD, frequent meetings were organized between the psychologists and the psychiatrist in charge of supervising the whole process to discuss cases and harmonize decisions. Responses and quotations were then entered in an electronic Case Report Form that was processed by a data manager through a database management system to ensure that data were adequately managed, organized, and standardized.

All exposed participants met DSM-5 criterion A, indicating that they experienced a traumatic event. Exposed participants were diagnosed with PTSD in its full form if all the additional diagnostic criteria defined by the DSM-5 were met: presence of intrusion (criterion B), avoidance (criterion C), negative alterations in mood or cognition (criterion D), arousal and reactivity symptoms (criterion E), with persistence of the symptoms superior to 1 month (criterion F) that caused significant distress and functional impairment (criterion G) and that are not due to medication, substance use, or other illness. Participants were diagnosed with PTSD in its partial form if they had significant and persistent reexperiencing symptoms (criterion B, G, F, and H) (38, 108). Trauma-exposed participants with full and partial PTSD profiles were grouped together for the purpose of statistical analyses in one unique clinical group referred to as the PTSD$^+$ group (38, 44). In addition, other life events were also scanned during the interview with the clinician. In the rare cases for which a traumatic event was present in a nonexposed individual ($N = 11$), the clinician administered the SCID to evaluate the presence or absence of PTSD symptoms. Following this procedure, only one nonexposed participant showed PTSD and was subsequently excluded from the study.

To further validate the SCID diagnosis, we additionally performed concurrent, convergent, predictive, and discriminant validity analyses of the PTSD$^+$ diagnosis. We used the various psychopathological scales at our disposal and performed a logistic regression analysis between the scores of those scales and the binary diagnosis (PTSD present versus absent). For concurrent validity, we used the PTSD checklist version DSM-5 (PCL-5) scale. For convergent analysis, we used the scales reflecting psychological distress or well-known comorbidities, including the Beck Depression Inventory scale, the State-Trait Anxiety Inventory, and the Ruminative Responses Scale. For predictive validity, we used the World Health Organization Well-Being Index and the Insomnia Severity Index. Last, to ensure that PTSD diagnosis was not confused with substance use abuse (discriminant analysis), we used the Alcohol Use Disorders Identification Test and Benzodiazepine Cognitive Attachment Scale. These analyses reveal that the diagnosis

of PTSD has significant concurrent and convergent validities for all dimensions tested and both time points. The diagnosis was also not related to substance use and has good discriminant validity. Results of these analyses as well as psychometric properties of the SCID are presented in the Supplementary Text.

At time 1, from the 114 included exposed participants, 52 individuals were resilient and were not diagnosed with PTSD (i.e., PTSD$^-$). Forty-six and 39 PTSD$^-$ participants had exploitable fMRI and hippocampal subfields data, respectively. Sixty-two individuals were diagnosed with PTSD in its partial or complete form (PTSD$^+$). Fifty-five and 53 PTSD$^+$ participants had exploitable fMRI and hippocampal subfields data, respectively. Seven exposed participants were excluded for non-respect of inclusion criteria. From the 80 nonexposed participants included, 72 and 56 had exploitable fMRI and hippocampal subfields data, respectively. Participants were excluded from the fMRI analyses due to the absence of intrusion rating owing to technical or behavioral issues, artifacts in the MRI images, or inability to pursue the experiment. Exclusions from the hippocampal subfields analyses were made for the following reasons: no acquisition of high-resolution images, MRI artifacts, or motion artifacts (anatomical landmarks used for segmentation not visible).

All the participants included at time 1 were asked to join the second phase of the study (time 2). Seventy-two of the 80 nonexposed participants and 100 of the 114 exposed participants joined the second phase. Exposed participants were once again diagnosed for PTSD in its partial or full form using DSM-5 (SCID) (107). Of the 100 included exposed participants at time 2, 43 individuals were classified as "stable PTSD$^-$" and were not diagnosed as PTSD across both time points (i.e., PTSD$^-$). Forty-two and 38 of those individuals had exploitable fMRI and hippocampal subfields data at time 2, respectively. Nineteen individuals were diagnosed with PTSD in its partial or complete form at time 1 (PTSD$^+$) but did not present any symptom at time 2 and were categorized as "remitted PTSD." Eighteen and 18 remitted PTSD participants had exploitable fMRI and hippocampal subfields data, respectively. Thirty-four individuals were diagnosed with PTSD in its partial or complete form across both time points and were categorized as "chronic PTSD." Thirty-four and 30 individuals with chronic PTSD had exploitable fMRI and hippocampal subfields data, respectively. Four non-PTSD participants at time 1 reached criteria for full or partial PTSD at time 2 and were discarded from further analyses. Details of the participants' demographic information are reported in Table 1.

We also asked participants if they were engaged for more than a week in any of the following treatments: (i) psychodynamic approach, (ii) cognitive behavioral therapy, (iii) eye movement desensitization and reprocessing, (iv) meditation, (v) simple interview, and (vi) psychotropic treatment. Seventy-seven percent of stable PTSD$^-$ (i.e., resilient) were engaged in one of those treatments, while 100 and 95% of remitted and chronic PTSD were. Critically, the proportion of individuals following treatments was not significantly different between remitted and chronic PTSD ($\chi^2 = 1.1615$, $P = 0.28$). The perceived efficacy of received treatment did not differ between those two groups ($T_{51} = -0.12$, $P = 0.9$). This suggests that PTSD remission cannot be solely accounted for by whether they received treatment or not.

All the participants of the two phases of the study were asked to join a clinical follow-up in 2020, 5 years after the terrorist attacks (time 3). This third phase included a telephonic assessment of symptoms severity through PCL-5 (51). At time 3, we were able to collect

Table 1. Participants' information.

		N total	N hippocampus	N fMRI	Age	Sex (M)	Total PCL
Time 1	Nonexposed	80	56	72	33.89 ± 11.32	37	4.91 ± 6.66
	PTSD⁻	52	39	46	36.83 ± 6.95	32	13.92 ± 11.47
	PTSD⁺	62	53	55	37.06 ± 8.17	27	37.79 ± 13.68
Time 2	Nonexposed	72	57	67	35.55 ± 11.33	33	2.79 ± 5.33
	Stable PTSD⁻	43	38	42	38.59 ± 7.37	28	9.88 ± 9.84
	Remitted PTSD	19	18	18	39.95 ± 8.69	10	17.05 ± 13.48
	Chronic PTSD	34	30	34	38.64 ± 7.71	13	34.21 ± 12.86

clinical data for 58 nonexposed, 38 stable PTSD⁻, 17 remitted, and 29 chronic PTSD participants.

All the participants completed the first phase of the study between 13 June 2016 and 7 June 2017, the second phase of the study between July 2018 and June 2019, and the third phase of the study between 28 April 2020 and 8 May 2020. Participants were financially compensated for their participation in the study. The study was approved by the regional research ethics committee ("Comité de Protection des Personnes Nord-Ouest III," sponsor ID: C16-13, RCB ID: 2016-A00661-50, clinicaltrials.gov, registration number NCT02810197). All the participants gave written informed consent before participation, in agreement with French ethical guidelines. Participants were asked not to consume psychostimulants, drugs, or alcohol prior to or during the experimental period.

Material
All the participants performed the TNT task (*54*) at the two phases of the longitudinal study. The stimuli were three sets of four series of lists of 72 association pairs of names and pictures representing objects, composed of neutral abstract French words (*109*) and objects selected from the Bank of Standardized Stimuli (BOSS), respectively (*110*). For each set, four lists of 18 pairs were assigned to four conditions [think, no-think, baseline, and unprimed for the final priming test task after the TNT phase; (*38*)]. Eight fillers were also created for practice. The sets were counterbalanced across longitudinal sessions, and the lists of pairs within each set were presented in counterbalanced order across the conditions. The lists of words were matched on average naming latency, number of letters, and lexical frequency (*109*). The lists of objects were matched relative to the naming latency, familiarity and visual complexity levels, viewpoint, name and object agreement, and manipulability, as measured in the BOSS validation study (*110*). Stimuli were presented using the Psychophysics Toolbox implemented in MATLAB (The MathWorks). We used neutral material completely disconnected from the traumatic experience that enables us to investigate general memory control mechanisms and incidentally avoid ethical issues for the trauma-exposed group.

Procedure
Before MRI acquisition, participants learned 54 French neutral word-object pairs that were presented 5 s each. After the presentation of all pairs, the word cue for a given pair was presented on the screen for up to 4 s, and participants were asked whether they could recall and fully visualize the paired object. If so, three objects then appeared on the screen (one correct and two foils), and participants had up to 4 s to select which object was associated with the word cue. After each recognition test, the object correctly associated with the word appeared 2500 ms on the screen, and participants were asked to use this feedback to increase their knowledge of the pair. Pairs were learned through this test-feedback cycle procedure until either the learning criterion (at least 90% of correct responses) was reached or a maximum of six presentations was achieved. Once participants had reached the learning criterion, their memory was assessed for one last time using a final criterion test on all of the pairs but without giving any feedback on the response. No group differences were found on this final criterion test. Following this learning phase, pairs were divided into three lists of 18 pairs assigned to think, no-think, and baseline conditions for the TNT task. Participants were given the TNT phase instructions and a short TNT practice session before MRI acquisition to familiarize them to the task.

Following this TNT practice session, participants entered the MRI scanner. During the T1 structural acquisition, the complete list of learned pairs was presented once again to reinforce the learning of the pairs (5 s for each pair). This overtraining procedure was intended to ensure that the word cue would automatically bring back the associated object. Following this reminder of the pairs, participants performed the TNT task, which was divided into four sessions of about 8 min each. In each session, the 18 think and 18 no-think items were presented twice. Word cues appeared for 3 s on the screen and were written either in green for think trials or in red for no-think trials. During the TNT practice session, participants were trained to use a direct suppression strategy. During the no-think trials, participants were instructed to imperatively prevent the object from coming to mind and to fixate and concentrate on the word cue without looking away. Participants were asked to block thoughts of the object by blanking their mind and to not replace the object with any other thoughts or mental images. If the object image came to mind anyway, then they were asked to push it out of mind. After the end of each of the think or no-think trial cues, participants reported whether the associated object had entered awareness by pressing one of two buttons corresponding to "yes" (i.e., even if the associated object pops very briefly into their mind) or "no." Although participants had up to 3600 ms to make this intrusion rating, they were instructed to make it quickly without thinking and dwelling too much about the associated object. The rating instruction was presented up to 1 s on the screen and followed by a jittered fixation cross (1400, 1800, 2000, 2200, or 2600 ms). The Genetic Algorithm toolbox (*111*) was used to optimize the

efficiency of the think–versus–no-think contrast. Twenty percent additional null events with no duration and followed by the jittered fixation cross only were added and were used to optimize the detection of the BOLD response against the rest. A perceptual identification task followed the TNT phase. Data about this task will be presented elsewhere.

MRI acquisition parameters
fMRI data were acquired on a 3-T Achieva scanner (Philips). At the two phases of the study, participants first underwent a high-resolution T1-weighted anatomical volume imaging using a three-dimensional (3D) fast field echo (FFE) sequence (3D-T1-FFE sagittal, repetition time (TR) of 20 ms, echo time (TE) of 4.6 ms, flip angle of 10°, SENSE factor of 2, 180 slices, voxels of 1 mm by 1 mm by 1 mm, no gap, field of view (FoV) of 256 mm by 256 mm by 180 mm, matrix of $256 \times 130 \times 180$). This acquisition was followed by the TNT functional sessions that were acquired using an ascending T2-star EPI sequence (MS-T2-star-FFE-EPI axial; TR of 2050 ms, TE of 30 ms, flip angle of 78°, 32 slices, slice thickness of 3 mm, gap of 0.75 mm, matrix of $64 \times 63 \times 32$, FoV of 192 mm by 192 mm by 119 mm, 235 volumes per run). Each of the four TNT functional sequences lasted about 8 min.

A high-resolution proton density-weighted sequence was also acquired perpendicularly to the long axis of the hippocampus (TR of 6500 ms, TE of 80 ms, flip angle of 90°, in-plane resolution of 0.391 mm by 0.391 mm, slice thickness of 2 mm, no gap, 30 slices) to segment hippocampal subfields.

fMRI preprocessing
The preprocessing of images was conducted with the Statistical Parametric Mapping toolbox (SPM 12, University College London, London, UK). Functional images collected during the TNT task of both longitudinal phases were (i) spatially realigned to correct for motion using default setting parameters provided by the batch mode and a six-parameter rigid body transformation, (ii) corrected for slice acquisition temporal delay using the middle temporal slice as reference, and (iii) coregistered with the skull-stripped structural image collected at time 1 using the mean fMRI image and the default setting parameters provided by the batch mode as estimation options. The T1-weighted anatomical volume was bias corrected and segmented using tissue probability maps for gray matter, white matter, and cerebrospinal fluid. The forward deformation field (y_*.nii) was derived from the nonlinear normalization of individual gray matter images collected at time 1 to the T1 template of the Montreal Neurological Institute (MNI). Deformation fields were estimated and applied using default setting parameters provided by the batch mode. Each point in this deformation field is a mapping between the MNI standard space and native-space coordinates in millimeter. Thus, this mapping was used to project the coordinates of the MNI standard space regions of interest (ROIs) to the native space functional images.

Computational modeling of the TNT task
We used meta-Bayesian computational modeling (112) to estimate participants' beliefs and related PEs about the probability of experiencing intrusive memories at the upcoming no-think trials. A detailed view of our computational approach can be found in our previous study that we conducted on the same dataset at time 1 (44). In this study, we fitted and compared different models to the binary

intrusion rating outputted by the TNT task, using the TAPAS toolbox (available at www.tnu.ethz.ch/de/software/tapas). Three different classes of perceptual models describing different hypotheses on how beliefs are updated were built and tested. The traditional Rescorla-Wagner model assumes a subject-specific static learning rate α that weights PE (113). The Kalman filter (114, 115) assumes that beliefs are uncertain and the learning rate, defined as the Kalman gain, is dynamically updated trial by trial with the modulation of two free parameters encoding beliefs uncertainty and reliability. Last, we included a two-level hierarchical Gaussian filter (HGF), hypothesizing that the learning underlying beliefs updating is dynamically modulated by trial-by-trial uncertainty (116). Such uncertainty is derived in a hierarchical fashion, considering the volatility of the environment on perceptual inference. In this previous study (44), Bayesian model selection and further model validations using parameter recovery, model recovery, and model falsification analyses revealed that this HGF model best accounted for intrusive rating during the TNT task. We therefore used the exact same HGF model in the current study, to estimate the participants' trial-wise beliefs and related PEs about the probability of experiencing intrusive memories. At a first level of the HGF model, participants would form beliefs, or predictions (x_1), about the probability of experiencing intrusive memories at the upcoming trial

$$x_1^{(t)} \sim \text{Bernoulli}\left(\frac{1}{\left\{1 + \exp\left[-x_2^{(t)}\right]\right\}}\right)$$

These beliefs are the logistic transformation of the second level x_2, which encodes beliefs about the volatility of memory intrusions experienced throughout the TNT task

$$x_2^{(t)} \sim N\left[x_2^{(t-1)}, \exp(\omega)\right]$$

At this level, beliefs are described by a Gaussian probability distribution whose variance encodes beliefs' uncertainty and is controlled by the free parameter ω. The HFG postulates that belief updating is driven by the uncertainty weighting of PE, such that PE induces greater learning when beliefs are uncertain.

To transform belief into intrusion rating, we built different response models, hypothesizing different sources of beliefs. Perceptual models were built using the total trial history throughout the TNT task as behavioral inputs and outputs (state models). Similarly, we built a distinct perceptual model for each word-object association pair (i.e., each item). Item models were built using the intrusion ratings related to each association pair (up to 18 different items), including eight repetitions in total for each item. After estimating these different perceptual models for each item, the inferred beliefs resulting from each of them were concatenated. Beliefs were mapped into intrusion ratings using a β density probability distribution as observation model as follows

$$p(y \mid \theta) = \frac{\Gamma(\alpha + \beta)}{\Gamma(\alpha)\Gamma(\beta)} y^{(\alpha-1)} (1 - y)^{(\beta-1)}$$

where θ refers to participants' beliefs estimated through the different perceptual models, Γ expresses a Gamma function, $\alpha = \theta \times \nu$, $\beta = \nu - \alpha$, and ν is a participant-specific free parameter (i.e., inverse decision noise regulating beta density width, estimated during model fit). This observation model described the accuracy of internal beliefs in

mapping onto the outcomes (i.e., intrusions). We wanted to compare the accuracy of different beliefs trajectories to establish the most likely source. Specifically, we built three different models assuming different sources of beliefs:

- The state source model hypothesized that belief θ at trial t was influenced by previous trial history, irrespective of the content of the specific item.

- The item source model hypothesized that belief θ was influenced exclusively by the specific word-object association pair, regardless of the previous trial history.

- The combined model hypothesized that participants combined state and item beliefs trajectories to improve prediction accuracy. Belief was created by a joint posterior distribution with mean $\hat{\mu}_c$, by summing beliefs arising from trial history and beliefs arising from the history of each specific item, weighted by their specific precisions and dividing the result by the sum of their variances

$$\theta = \hat{\mu}_c = \frac{\hat{\mu}_s \hat{\pi}_s + \hat{\mu}_i \hat{\pi}_i}{\hat{\pi}_s + \hat{\pi}_i}$$

In our previous study (44), results showed that the combined HGF outperformed other models. We therefore used this model to estimate beliefs and PE for the longitudinal analysis of the current study.

Computational dynamic causal modeling

DCM allows creating and comparing different hypothesis-driven generative models to infer the effective connectivity between a set of predefined brain regions. The construction of the generative model relies on the manipulation of three matrices: The A matrix encodes the intrinsic connectivity, the B matrix encodes the modulation of experimental conditions over connectivity, and the C matrix encodes the modulation experimental conditions over the activity of single brain regions (117).

DCM entails a priori definition of ROIs. To be able to analyze the longitudinal change of DCM coupling parameters, we used the exact same ROIs and model space than in our previous study conducted at time 1 (codes available on https://github.com/PierreGagnepain/predictive_control). The ROIs included the anterior and posterior parts of the MFG (aMFG and pMFG, respectively), given their role in memory suppression (41, 42, 118), the rostral and caudal hippocampus (rHIP and cHIP, respectively), and the precuneus (PC). We first selected the ROIs from the Brainnetome Atlas (119) (http://atlas.brainnetome.org/). The aMFG region included A46 (center coordinates: $x = 28$, $y = 55$, $z = 17$) and A9/46v ($x = 42$, $y = 44$, $z = 14$), pMFG included A9/46d ($x = 30$, $y = 37$, $z = 36$) and A8vl ($x = 42$, $y = 27$, $z = 39$), rHIP and cHIP corresponded to two ROIs ($x = 22$, $y = -12$, $z = -20$ and $x = 29$, $y = -27$, $z = -10$), and PC corresponded to dorsomeidal parieto-occipital sulcus ($x = 16$, $y = -64$, $z = 25$). The MNI coordinates of the five ROIs were projected onto participants' native space using the deformation field, without any spatial warping or smoothing of the functional images, to ensure maximum accuracy. However, for there to be sufficient demarcation between the aMFG and pMFG signals, aMFG coordinates were initially limited to y > 35 mm and pMFG coordinates to $y < 25$ mm.

At time 1, for the DCM analysis, we identified for each participant the maximum activation peak within the ROIs (using no-think > think contrast for aMFG and pMFG and no-think < think contrast for memory regions). We then created for each participant a

mask of the most significant 30 contiguous voxels (1012.5 mm^3), derived from the individual statistical map of the main effect of suppression, and then summarized the voxel time series within this mask. We used a similar procedure for the analyses at time 2. To increase the comparability of time 1 and time 2, we started from the same peak identified at time 1 and grew a region of 30 contiguous voxels according to the individual statistical map. This procedure ensures that the time courses of fMRI activity used for DCM originated from the same center while preserving the selection of most activated voxels.

The main goal of our DCM analyses was to model predictive control and reactive control of intrusive memories. The model space in our initial study conducted at time 1 was composed of four main families of models (120). The "computational top-down modulation" family postulates the existence of predictive and reactive mechanisms, by assuming that beliefs and PE, respectively, parametrically modulate the connectivity from aMFG and pMFG to the hippocampus and the PC. This family can be divided into two subfamilies: one hypothesizing that aMFG is involved in reactive control and the pMFG in predictive control, and another hypothesizing the opposite involvement. To validate the meaningfulness of predictive control and reactive control, we also included a "no computation" model family in which top-down coupling was modulated by no-think items without further parametric modulation on this input and a "computational bottom-up modulation" model family in which the influence of computational parameters arises from memory to control regions. Last, a null model family, in which no connections were modulated, was also designed [see (44) for more details]. The random-effects Bayesian model selection (121) conducted during this first study revealed that the computational top-down modulation family outperformed the others. Critically, this finding was observed across the whole population of participants, without further differences in the preferred model architecture across the groups of participants. Within this family, however, we did not have evidence for a preferential involvement of aMFG and pMFG in either predictive control or reactive control. Therefore, a single parameter reflecting the top-down control associated with each form of computation (i.e., predictive and reactive) was summarized using Bayesian model averaging (BMA) (120) across all the models of this family. For time 2, the exact same BMA procedure was applied within the same family of models. At time 1, the aggregation of coupling parameters modulating the two hippocampal regions included in our DCMs revealed a significant Group*Control interactions when individuals with PTSD were compared to exposed without PTSD or to nonexposed individuals. This interaction was absent with respect to the precuneus. We therefore focus the current longitudinal study on the same top-down coupling parameter, reflecting the regulation of hippocampal activity by the MFG.

Imbalance analysis

We projected neurocomputational markers of predictive control (PC) and reactive control (RC) of intrusive memories onto two orthogonal axes of a polar coordinate system. Angular coordinates were expressed in degrees between −180° and + 180°, with a 0° reference point at the bottom of the y axis (i.e., 0° to 180° anticlockwise and 0° to −180° clockwise). The first axis (+45° to −135°) represented PC. Negative PC coupling values were projected on the +45° direction, and positive PC coupling parameters onto the opposite −135° direction. The second axis (+135° to −45°) represented

RC. Negative RC coupling values were projected onto the −45° direction, and positive RC coupling parameters onto the opposite +135° direction.

For each participant, we calculated the resultant force (RF) combining predictive and reactive forces. The RF represents the vector sum of a set of forces. Given two forces F_{PC} and F_{RC}, characterized by known angles α_1 and α_2 from 0° on the y axis of a circle and the x and y Cartesian components (Fx_{PC}, Fx_{RC} and Fy_{PC}, Fy_{RC}), the RF's Cartesian components can be obtained as follows

$$F_{Rx} = Fx_{PC} + Fx_{RC}$$

$$F_{Ry} = Fy_{PC} + Fy_{RC}$$

In our analyses, we focused on the RF's direction, not its magnitude. The RF represents the summative effect of predictive and reactive vectors of force. As the two forces were applied in different directions yet both pointing downward, the 0° position represented the equilibrium point. The more the RF approached the 0° direction, the more balanced the two forces were. To obtain an imbalance angle (IB) for each participant, we computed the angle θ between the RF and the 0° position using trigonometry

$$IB = \theta = \left(\frac{F_{Ry}}{F_{Rx}} \right)$$

Both predictive and reactive negative coupling parameters reflected downward yet orthogonal forces, originating from the same point of application. This illustrates how a unique control system may suppress memory processing according to two independent but complementary processes serving the same function.

Hippocampal subfield segmentation

Hippocampal subfields were automatically segmented using the ASHS software (*122*), using a procedure previously validated in the same cohort at time 1 (*50*). Using the high-resolution proton density–weighted sequence acquired perpendicularly to the long axis of the hippocampus at time 1, we created an atlas package on a subsample ($n = 22$) of participants, using the ASHS training pipeline (instructions on https://sites.google.com/view/ashs-dox/local-ashs/building-an-atlas-for-t2-mri). We first manually segmented the scans of 22 participants at time 1 (7 healthy controls, 7 PTSD⁻, and 8 PTSD⁺), following a procedure developed in our laboratory (*52*, *53*). From the most anterior part of the hippocampus to the colliculi, the hippocampus was segmented into three subregions: subiculum; CA1; and a region combining CA2, CA3, and the DG (CA2-3/DG). Segmenting the individual CA2, CA3, and DG subfields is inaccurate, unreliable, and difficult, owing to the absence of useful anatomical landmarks and the very small size of CA2 and CA3 (*52*, *53*). Therefore, these regions were combined into a single subregion. Once the atlas package had been created, we assessed the accuracy of ASHS automated segmentation (relative to manual segmentation) with the subsample of 22 participants, using leave-one-out cross-validations (*123*). ASHS automatically segmented the images of the remaining participants. Automatic segmentations were all visually checked before we extracted the volumes for statistical analysis. The details about the validation and reliability of this procedure and segmentation protocol are reported in Postel *et al.* (*50*). This previous study revealed no significant interactions with hemispheres.

We therefore averaged left and right volumes for the current longitudinal study.

Statistical analyses
Group*Time interactions

All analyses were conducted using LME models, which are especially recommended for the analysis of longitudinal design, using the fitlme function of MATLAB (The MathWorks). Fitting included all groups and both time points and was performed using the restricted maximum likelihood and the Cholesky parametrization for the covariance matrix. Time and group status, as well as their interactions, were set as fixed effects, and subjects' intercepts and longitudinal slopes were set as random effects to follow current guidelines for LME analysis (*7*). This approach considers inter-subjects' variability, by allowing subjects to have specific intercepts and evolution rates in time. Four LME analyses were performed: (i) analysis of intrusion slope (calculated by taking the Pearson correlation between the intrusion proportions and the eight repetitions in the suppression instruction across TNT sessions), (ii) analysis of the top-down modulation of hippocampal activity associated with the predictive and reactive suppression of intrusive memories, (iii) analysis of the volume of CA1, and (iv) of CA2-3/DG subfields. For the analysis of DCM coupling parameters, the effect of control (i.e., reactive versus predictive) was added both as a fixed effect of interest and as a random effect (i.e., accounting for inter-subject variability). For the analysis of hippocampal subfields, we also included sex, group-mean–centered age, and TIV as nuisance covariates to reduce unexplained variance of the hippocampal subfields' volumes. For all the models, fixed effects (i.e., time, group, and control) were coded as categorical variables, the coefficients for the first category were set to zero (i.e., "reference" dummy variable coding method, taking the nonexposed group at time 1 as the reference group), and appropriate contrasts for planned comparisons were then set accordingly to compare the different groups or conditions. Degrees of freedom were corrected using the Satterthwaite correction. To test for the main hypotheses associated with this study regarding (i) the presence of a Control*Time interaction in the remitted group associated DCM coupling parameters and (ii) the presence of a Time effect in the chronic PTSD group regarding hippocampal volumes, we adjusted the P value with respect to the number of groups using fdr correction given that we repeated the same contrast for each group separately. When we performed further planned comparisons within a groups (e.g., within Control*Time interaction for DCM), we adjusted the P value for the number of comparisons that were made.

Longitudinal effects

We also investigated how interindividual variations in longitudinal changes between time 1 and time 2, in the balance of control processes, or hippocampal volumes were related to the clinical evolution of individuals with chronic PTSD between time 2 and time 3. To isolate longitudinal changes, the cross-sectional effect reflecting interindividual variations (i.e., the mean between time 1 and time 2) was subtracted from each data point. The independent variable, therefore, reflected longitudinal changes orthogonalized to the mean [see (*57*) for a similar procedure to isolate the influence of longitudinal and cross-sectional effects]. Cross-sectional effects and their interaction with longitudinal changes were also included in the LME model to reduce unexplained variance. Those changes were compared to the intrusive reexperiencing and avoidance severity scores of the PTSD Checklist for DSM-5 collected at time 2 and time 3, to forecast

upcoming clinical changes using the evolution of memory control and hippocampal markers between time 1 and time 2. Degrees of freedom were corrected using the Satterthwaite correction. We adjusted the P value for the number of symptoms tested using fdr. Note that the same analysis was performed using the longitudinal and cross-sectional effects of imbalance in control as independent variables and the volumes of the hippocampus at time 1 and time 2 as dependent variables.

Imbalance analysis

For this complementary analysis, we used the Circular Statistics toolbox in MATLAB (*124*). Groups*Time interaction was performed using the parametric two-way ANOVA for circular data (i.e., circ_hktest function). Group comparisons within time points were performed using Watson's two-sample tests, a nonparametric version of the two-sample *t* test for circular data (i.e., circ_wwtest function).

Supplementary Materials

This PDF file includes:
Supplementary Text
Tables S1 and S2
References

REFERENCES AND NOTES

1. R. Kalisch, D. G. Baker, U. Basten, M. P. Boks, G. A. Bonanno, E. Brummelman, A. Chmitorz, G. Fernàndez, C. J. Fiebach, I. Galatzer-Levy, E. Geuze, S. Groppa, I. Helmreich, T. Hendler, E. J. Hermans, T. Jovanovic, T. Kubiak, K. Lieb, B. Lutz, M. B. Müller, R. J. Murray, C. M. Nievergelt, A. Reif, K. Roelofs, B. P. F. Rutten, D. Sander, A. Schick, O. Tüscher, I. Van Diest, A.-L. van Harmelen, I. M. Veer, E. Vermetten, C. H. Vinkers, T. D. Wager, H. Walter, M. Wessa, M. Wibral, B. Kleim, The resilience framework as a strategy to combat stress-related disorders. *Nat. Hum. Behav.* **1**, 784–790 (2017).
2. A. Pascual-Leone, D. Bartres-Faz, Human brain resilience: A call to action. *Ann. Neurol.* **90**, 336–349 (2021).
3. S. J. Russo, J. W. Murrough, M.-H. Han, D. S. Charney, E. J. Nestler, Neurobiology of resilience. *Nat. Neurosci.* **15**, 1475–1484 (2012).
4. S. J. H. van Rooij, J. L. Santos, C. A. Hinojosa, T. D. Ely, N. G. Harnett, V. P. Murty, L. A. M. Lebois, T. Jovanovic, S. L. House, S. E. Bruce, F. L. Beaudoin, X. An, T. C. Neylan, G. D. Clifford, S. D. Linnstaedt, L. T. Germine, K. A. Bollen, S. L. Rauch, J. P. Haran, A. B. Storrow, C. Lewandowski, P. I. Musey, P. L. Hendry, S. Sheikh, C. W. Jones, B. E. Punches, R. A. Swor, J. L. Pascual, M. J. Seamon, E. Harris, C. Pearson, D. A. Peak, R. C. Merchant, R. M. Domeier, N. K. Rathlev, B. J. O'Neil, L. D. Sanchez, J. Joormann, D. A. Pizzagalli, J. F. Sheridan, S. E. Harte, R. C. Kessler, K. C. Koenen, S. A. McLean, K. J. Ressler, J. S. Stevens, Defining the *r* factor for post-trauma resilience and its neural predictors. *Nat. Ment. Health* **2**, 680–693 (2024).
5. R. Yehuda, J. LeDoux, Response variation following trauma: A translational neuroscience approach to understanding PTSD. *Neuron* **56**, 19–32 (2007).
6. A. R. Roeckner, K. I. Oliver, L. A. M. Lebois, S. J. H. van Rooij, J. S. Stevens, Neural contributors to trauma resilience: A review of longitudinal neuroimaging studies. *Transl. Psychiatry* **11**, 508 (2021).
7. N. Kitayama, V. Vaccarino, M. Kutner, P. Weiss, J. D. Bremner, Magnetic resonance imaging (MRI) measurement of hippocampal volume in posttraumatic stress disorder: A meta-analysis. *J. Affect. Disord.* **88**, 79–86 (2005).
8. M. W. Logue, S. J. H. van Rooij, E. L. Dennis, S. L. Davis, J. P. Hayes, J. S. Stevens, M. Densmore, C. C. Haswell, J. Ipser, S. B. J. Koch, M. Korgaonkar, L. A. M. Lebois, M. Peverill, J. T. Baker, P. S. W. Boedhoe, J. L. Frijling, S. A. Gruber, I. Harpaz-Rotem, N. Jahanshad, S. Koopowitz, I. Levy, L. Nawijn, L. O'Connor, M. Olff, D. H. Salat, M. A. Sheridan, J. M. Spielberg, M. van Zuiden, S. R. Winternitz, J. D. Wolff, E. J. Wolf, X. Wang, K. Wrocklage, C. G. Abdallah, R. A. Bryant, E. Geuze, T. Jovanovic, M. L. Kaufman, A. P. King, J. H. Krystal, J. Lagopoulos, M. Bennett, R. Lanius, I. Liberzon, R. E. McGlinchey, K. A. McLaughlin, W. P. Milberg, M. W. Miller, K. J. Ressler, D. J. Veltman, D. J. Stein, K. Thomaes, P. M. Thompson, R. A. Morey, Smaller hippocampal volume in posttraumatic stress disorder: A multisite ENIGMA-PGC study: Subcortical volumetry results from posttraumatic stress disorder consortia. *Biol. Psychiatry* **83**, 244–253 (2018).
9. D. C. M. O'Doherty, K. M. Chitty, S. Saddiqui, M. R. Bennett, J. Lagopoulos, A systematic review and meta-analysis of magnetic resonance imaging measurement of structural volumes in posttraumatic stress disorder. *Psychiatry Res. Neuroimaging* **232**, 1–33 (2015).
10. R. J. Fenster, L. A. M. Lebois, K. J. Ressler, J. Suh, Brain circuit dysfunction in post-traumatic stress disorder: From mouse to man. *Nat. Rev. Neurosci.* **19**, 535–551 (2018).
11. H. K. Lambert, K. A. McLaughlin, Impaired hippocampus-dependent associative learning as a mechanism underlying PTSD: A meta-analysis. *Neurosci. Biobehav. Rev.* **107**, 729–749 (2019).
12. S. A. Joshi, E. R. Duval, B. Kubat, I. Liberzon, A review of hippocampal activation in post-traumatic stress disorder. *Psychophysiology* **57**, e13357 (2020).
13. I. Liberzon, J. L. Abelson, Context processing and the neurobiology of post-traumatic stress disorder. *Neuron* **92**, 14–30 (2016).
14. S. Lissek, B. van Meurs, Learning models of PTSD: Theoretical accounts and psychobiological evidence. *Int. J. Psychophysiol.* **98**, 594–605 (2015).
15. S. Kida, Reconsolidation/destabilization, extinction and forgetting of fear memory as therapeutic targets for PTSD. *Psychopharmacology (Berl)* **236**, 49–57 (2019).
16. A. Desmedt, A. Marighetto, P.-V. Piazza, Abnormal fear memory as a model for posttraumatic stress disorder. *Biol. Psychiatry* **78**, 290–297 (2015).
17. A. S. Al Abed, E.-G. Ducourneau, C. Bouarab, A. Sellami, A. Marighetto, A. Desmedt, Preventing and treating PTSD-like memory by trauma contextualization. *Nat. Commun.* **11**, 4220 (2020).
18. R. Admon, M. R. Milad, T. Hendler, A causal model of post-traumatic stress disorder: Disentangling predisposed from acquired neural abnormalities. *Trends Cogn. Sci.* **17**, 337–347 (2013).
19. A. Ehlers, D. M. Clark, A cognitive model of posttraumatic stress disorder. *Behav. Res. Ther.* **38**, 319–345 (2000).
20. C. R. Brewin, J. D. Gregory, M. Lipton, N. Burgess, Intrusive images in psychological disorders: Characteristics, neural mechanisms, and treatment implications. *Psychol. Rev.* **117**, 210–232 (2010).
21. H. van Marle, PTSD as a memory disorder. *Eur. J. Psychotraumatol.* **6**, 27633 (2015).
22. R. A. Bryant, M. Creamer, M. O'Donnell, D. Forbes, A. C. McFarlane, D. Silove, D. Hadzi-Pavlovic, Acute and chronic posttraumatic stress symptoms in the emergence of posttraumatic stress disorder: A network analysis. *JAMA Psychiatry* **74**, 135–142 (2017).
23. A. Sekiguchi, M. Sugiura, Y. Taki, Y. Kotozaki, R. Nouchi, H. Takeuchi, T. Araki, S. Hanawa, S. Nakagawa, C. M. Miyauchi, A. Sakuma, R. Kawashima, Brain structural changes as vulnerability factors and acquired signs of post-earthquake stress. *Mol. Psychiatry* **18**, 618–623 (2013).
24. S. J. H. van Rooij, M. Kennis, R. Sjouwerman, M. P. van den Heuvel, R. S. Kahn, E. Geuze, Smaller hippocampal volume as a vulnerability factor for the persistence of post-traumatic stress disorder. *Psychol. Med.* **45**, 2737–2746 (2015).
25. L. Lindgren, J. Bergdahl, L. Nyberg, Longitudinal evidence for smaller hippocampus volume as a vulnerability factor for perceived stress. *Cereb. Cortex* **26**, 3527–3533 (2016).
26. M. W. Gilbertson, M. E. Shenton, A. Ciszewski, K. Kasai, N. B. Lasko, S. P. Orr, R. K. Pitman, Smaller hippocampal volume predicts pathologic vulnerability to psychological trauma. *Nat. Neurosci.* **5**, 1242–1247 (2002).
27. S. B. J. Koch, V. A. van Ast, R. Kaldewaij, M. M. Hashemi, W. Zhang, F. Klumpers, K. Roelofs, Larger dentate gyrus volume as predisposing resilience factor for the development of trauma-related symptoms. *Neuropsychopharmacology* **46**, 1283–1292 (2021).
28. O. Bonne, D. Brandes, A. Gilboa, J. M. Gomori, M. E. Shenton, R. K. Pitman, A. Y. Shalev, Longitudinal MRI study of hippocampal volume in trauma survivors with PTSD. *Am. J. Psychiatry* **158**, 1248–1251 (2001).
29. S. A. Heyn, T. J. Keding, M. C. Ross, J. M. Cisler, J. A. Mumford, R. J. Herringa, Abnormal prefrontal development in pediatric posttraumatic stress disorder: A longitudinal structural and functional magnetic resonance imaging study. *Biol. Psychiatry Cogn. Neurosci. Neuroimaging* **4**, 171–179 (2019).
30. Z. Ben-Zion, N. Korem, T. R. Spiller, O. Duek, J. N. Keynan, R. Admon, I. Harpaz-Rotem, I. Liberzon, A. Y. Shalev, T. Hendler, Longitudinal volumetric evaluation of hippocampus and amygdala subregions in recent trauma survivors. *Mol. Psychiatry* **28**, 657–667 (2023).
31. C. N. Weis, E. K. Webb, A. A. Huggins, M. Kallenbach, T. A. Miskovich, J. M. Fitzgerald, K. P. Bennett, J. L. Krukowski, T. A. deRoon-Cassini, C. L. Larson, Stability of hippocampal subfield volumes after trauma and relationship to development of PTSD symptoms. *Neuroimage* **236**, 118076 (2021).
32. R. M. Sapolsky, Chickens, eggs and hippocampal atrophy. *Nat. Neurosci.* **5**, 1111–1113 (2002).
33. B. S. McEwen, C. Nasca, J. D. Gray, Stress effects on neuronal structure: Hippocampus, amygdala, and prefrontal cortex. *Neuropsychopharmacology* **41**, 3–23 (2016).
34. S. J. H. van Rooij, M. Ravi, T. D. Ely, V. Michopoulos, S. J. Winters, J. Shin, M.-F. Marin, M. R. Milad, B. O. Rothbaum, K. J. Ressler, T. Jovanovic, J. S. Stevens, Hippocampal activation during contextual fear inhibition related to resilience in the early aftermath of trauma. *Behav. Brain Res.* **408**, 113282 (2021).
35. E. W. Dickie, A. Brunet, V. Akerib, J. L. Armony, Neural correlates of recovery from post-traumatic stress disorder: A longitudinal fMRI investigation of memory encoding. *Neuropsychologia* **49**, 1771–1778 (2011).

36. R. Admon, G. Lubin, O. Stern, K. Rosenberg, L. Sela, H. Ben-Ami, T. Hendler, Human vulnerability to stress depends on amygdala's predisposition and hippocampal plasticity. *Proc. Natl. Acad. Sci. U.S.A.* **106**, 14120–14125 (2009).

37. S. J. H. van Rooij, J. S. Stevens, T. D. Ely, R. Hinrichs, V. Michopoulos, S. J. Winters, Y. E. Ogbonmwan, J. Shin, N. R. Nugent, L. A. Hudak, B. O. Rothbaum, K. J. Ressler, T. Jovanovic, The role of the hippocampus in predicting future posttraumatic stress disorder symptoms in recently traumatized civilians. *Biol. Psychiatry* **84**, 106–115 (2018).

38. A. Mary, J. Dayan, G. Leone, C. Postel, F. Fraisse, C. Malle, T. Vallée, C. Klein-Peschanski, F. Viader, V. de la Sayette, D. Peschanski, F. Eustache, P. Gagnepain, Resilience after trauma: The role of memory suppression. *Science* **367**, eaay8477 (2020).

39. B. J. Levy, M. C. Anderson, Purging of memories from conscious awareness tracked in the human brain. *J. Neurosci.* **32**, 16785–16794 (2012).

40. R. G. Benoit, J. C. Hulbert, E. Huddleston, M. C. Anderson, Adaptive top–down suppression of hippocampal activity and the purging of intrusive memories from consciousness. *J. Cogn. Neurosci.* **27**, 96–111 (2015).

41. P. Gagnepain, J. Hulbert, M. C. Anderson, Parallel regulation of memory and emotion supports the suppression of intrusive memories. *J. Neurosci.* **37**, 6423–6441 (2017).

42. P. Gagnepain, R. N. Henson, M. C. Anderson, Suppressing unwanted memories reduces their unconscious influence via targeted cortical inhibition. *Proc. Natl. Acad. Sci. U.S.A.* **111**, E1310–E1319 (2014).

43. M. C. Anderson, J. C. Hulbert, Active forgetting: Adaptation of memory by prefrontal control. *Annu. Rev. Psychol.* **72**, 1–36 (2021).

44. G. Leone, C. Postel, A. Mary, F. Fraisse, T. Vallée, F. Viader, V. de La Sayette, D. Peschanski, J. Dayan, F. Eustache, P. Gagnepain, Altered predictive control during memory suppression in PTSD. *Nat. Commun.* **13**, 3300 (2022).

45. L. Iyadurai, R. M. Visser, A. Lau-Zhu, K. Porcheret, A. Horsch, E. A. Holmes, E. L. James, Intrusive memories of trauma: A target for research bridging cognitive science and its clinical application. *Clin. Psychol. Rev.* **69**, 67–82 (2019).

46. H. G. Engen, M. C. Anderson, Memory control: A fundamental mechanism of emotion regulation. *Trends Cogn. Sci.* **22**, 982–995 (2018).

47. N. Legrand, O. Etard, A. Vandevelde, M. Pierre, F. Viader, P. Clochon, F. Doidy, D. Peschanski, F. Eustache, P. Gagnepain, Long-term modulation of cardiac activity induced by inhibitory control over emotional memories. *Sci. Rep.* **10**, 15008 (2020).

48. B. E. Depue, J. M. Orr, H. R. Smolker, F. Naaz, M. T. Banich, The organization of right prefrontal networks reveals common mechanisms of inhibitory regulation across cognitive, emotional, and motor processes. *Cereb. Cortex* **26**, 1634–1646 (2016).

49. Z. Mamat, M. C. Anderson, Improving mental health by training the suppression of unwanted thoughts. *Sci. Adv.* **9**, eadh5292 (2023).

50. C. Postel, A. Mary, J. Dayan, F. Fraisse, T. Vallée, B. Guillery-Girard, F. Viader, V. de La Sayette, D. Peschanski, F. Eustache, P. Gagnepain, Variations in response to trauma and hippocampal subfield changes. *Neurobiol. Stress* **15**, 100346 (2021).

51. B. Konecky, E. C. Meyer, N. A. Kimbrel, S. B. Morissette, The structure of *DSM-5* posttraumatic stress disorder symptoms in war veterans. *Anxiety Stress Coping* **29**, 497–506 (2016).

52. R. de Flores, R. La Joie, B. Landeau, A. Perrotin, F. Mézenge, V. de La Sayette, F. Eustache, B. Desgranges, G. Chételat, Effects of age and Alzheimer's disease on hippocampal subfields: Comparison between manual and freesurfer volumetry. *Hum. Brain Mapp.* **36**, 463–474 (2015).

53. R. La Joie, M. Fouquet, F. Mézenge, B. Landeau, N. Villain, K. Mevel, A. Pélerin, F. Eustache, B. Desgranges, G. Chételat, Differential effect of age on hippocampal subfields assessed using a new high-resolution 3T MR sequence. *Neuroimage* **53**, 506–514 (2010).

54. M. C. Anderson, C. Green, Suppressing unwanted memories by executive control. *Nature* **410**, 366–369 (2001).

55. N. Legrand, O. Etard, F. Viader, P. Clochon, F. Doidy, F. Eustache, P. Gagnepain, Attentional capture mediates the emergence and suppression of intrusive memories. *iScience* **25**, 105516 (2022).

56. A. F. T. Arnsten, Stress signalling pathways that impair prefrontal cortex structure and function. *Nat. Rev. Neurosci.* **10**, 410–422 (2009).

57. M. M. Vaghi, M. Moutoussis, F. Váša, R. A. Kievit, T. U. Hauser, P. E. Vértes, N. Shahar, R. Romero-Garcia, M. G. Kitzbichler, E. T. Bullmore, NSPN Consortium, R. J. Dolan, Compulsivity is linked to reduced adolescent development of goal-directed control and frontostriatal functional connectivity. *Proc. Natl. Acad. Sci. U.S.A.* **117**, 25911–25922 (2020).

58. C. D. Conrad, J. B. Ortiz, J. M. Judd, Chronic stress and hippocampal dendritic complexity: Methodological and functional considerations. *Physiol. Behav.* **178**, 66–81 (2017).

59. V. M. Heine, J. Zareno, S. Maslam, M. Joëls, P. J. Lucassen, Chronic stress in the adult dentate gyrus reduces cell proliferation near the vasculature and VEGF and Flk-1 protein expression. *Eur. J. Neurosci.* **21**, 1304–1314 (2005).

60. S. Brummelte, L. A. M. Galea, Chronic high corticosterone reduces neurogenesis in the dentate gyrus of adult male and female rats. *Neuroscience* **168**, 680–690 (2010).

61. J. E. Dunsmoor, J. M. Cisler, G. A. Fonzo, S. K. Creech, C. B. Nemeroff, Laboratory models of post-traumatic stress disorder: The elusive bridge to translation. *Neuron* **110**, 1754–1776 (2022).

62. E. J. Kim, B. Pellman, J. J. Kim, Stress effects on the hippocampus: A critical review. *Learn. Mem.* **22**, 411–416 (2015).

63. T. J. Schoenfeld, E. Gould, Stress, stress hormones, and adult neurogenesis. *Exp. Neurol.* **233**, 12–21 (2012).

64. S. J. Lupien, R.-P. Juster, C. Raymond, M.-F. Marin, The effects of chronic stress on the human brain: From neurotoxicity, to vulnerability, to opportunity. *Front. Neuroendocrinol.* **49**, 91–105 (2018).

65. T. Lee, T. Jarome, S.-J. Li, J. J. Kim, F. J. Helmstetter, Chronic stress selectively reduces hippocampal volume in rats: A longitudinal MRI study. *Neuroreport* **20**, 1554–1558 (2009).

66. E. J. Kim, J. J. Kim, Neurocognitive effects of stress: A metaparadigm perspective. *Mol. Psychiatry* **28**, 2750–2763 (2023).

67. A. Surget, C. Belzung, Adult hippocampal neurogenesis shapes adaptation and improves stress response: A mechanistic and integrative perspective. *Mol. Psychiatry* **27**, 403–421 (2022).

68. C. D. Conrad, What is the functional significance of chronic stress-induced CA3 dendritic retraction within the hippocampus? *Behav. Cogn. Neurosci. Rev.* **5**, 41–60 (2006).

69. D. N. Abrous, M. Koehl, M. Lemoine, A Baldwin interpretation of adult hippocampal neurogenesis: From functional relevance to physiopathology. *Mol. Psychiatry* **27**, 383–402 (2022).

70. F. Cathomas, J. W. Murrough, E. J. Nestler, M.-H. Han, S. J. Russo, Neurobiology of resilience: Interface between mind and body. *Biol. Psychiatry* **86**, 410–420 (2019).

71. A. Besnard, A. Sahay, Adult hippocampal neurogenesis, fear generalization, and stress. *Neuropsychopharmacology* **41**, 24–44 (2016).

72. M. C. Anderson, S. B. Floresco, Prefrontal-hippocampal interactions supporting the extinction of emotional memories: The retrieval stopping model. *Neuropsychopharmacology* **47**, 180–195 (2022).

73. R. Kaldewaij, S. B. J. Koch, M. M. Hashemi, W. Zhang, F. Klumpers, K. Roelofs, Anterior prefrontal brain activity during emotion control predicts resilience to post-traumatic stress symptoms. *Nat. Hum. Behav.* **5**, 1055–1064 (2021).

74. A. Ehlers, A. Hackmann, T. Michael, Intrusive re-experiencing in post-traumatic stress disorder: Phenomenology, theory, and therapy. *Memory* **12**, 403–415 (2004).

75. C. P. McLean, E. B. Foa, Emotions and emotion regulation in posttraumatic stress disorder. *Curr. Opin. Psychol.* **14**, 72–77 (2017).

76. A. Hackmann, A. Ehlers, A. Speckens, D. M. Clark, Characteristics and content of intrusive memories in PTSD and their changes with treatment. *J. Trauma. Stress* **17**, 231–240 (2004).

77. M. W. Miller, A. P. Lin, E. J. Wolf, D. R. Miller, Oxidative stress, inflammation, and neuroprogression in chronic PTSD. *Harv. Rev. Psychiatry* **26**, 57–69 (2018).

78. S. Schumacher, H. Niemeyer, S. Engel, J. C. Cwik, S. Laufer, H. Klusmann, C. Knaevelsrud, HPA axis regulation in posttraumatic stress disorder: A meta-analysis focusing on potential moderators. *Neurosci. Biobehav. Rev.* **100**, 35–57 (2019).

79. L. Y. Maeng, M. R. Milad, Post-traumatic stress disorder: The relationship between the fear response and chronic stress. *Chronic Stress* **1**, 2470547017713297 (2017).

80. J. Cheung, B. Garber, R. A. Bryant, The role of stress during memory reactivation on intrusive memories. *Neurobiol. Learn. Mem.* **123**, 28–34 (2015).

81. C. E. Hilberdink, S. R. de Rooij, M. Olff, J. A. Bosch, M. van Zuiden, Acute stress reactivity and intrusive memory development: A randomized trial using an adjusted trauma film paradigm. *Psychoneuroendocrinology* **139**, 105686 (2022).

82. J.-Y. Zhang, T.-H. Liu, Y. He, H.-Q. Pan, W.-H. Zhang, X.-P. Yin, X.-L. Tian, B.-M. Li, X.-D. Wang, A. Holmes, T.-F. Yuan, B.-X. Pan, Chronic stress remodels synapses in an amygdala circuit–specific manner. *Biol. Psychiatry* **85**, 189–201 (2019).

83. C. Fee, T. Prevot, K. Misquitta, M. Banasr, E. Sibille, Chronic stress-induced behaviors correlate with exacerbated acute stress-induced cingulate cortex and ventral hippocampus activation. *Neuroscience* **440**, 113–129 (2020).

84. B. Czéh, Z. K. K. Varga, K. Henningsen, G. L. Kovács, A. Miseta, O. Wiborg, Chronic stress reduces the number of GABAergic interneurons in the adult rat hippocampus, dorsal-ventral and region-specific differences. *Hippocampus* **25**, 393–405 (2015).

85. A. Albrecht, E. Redavide, S. Regev-Tsur, O. Stork, G. Richter-Levin, Hippocampal GABAergic interneurons and their co-localized neuropeptides in stress vulnerability and resilience. *Neurosci. Biobehav. Rev.* **122**, 229–244 (2021).

86. M. Selten, H. van Bokhoven, N. Nadif Kasri, Inhibitory control of the excitatory/inhibitory balance in psychiatric disorders. *F1000Res* **7**, 23 (2018).

87. V. S. Sohal, J. L. R. Rubenstein, Excitation-inhibition balance as a framework for investigating mechanisms in neuropsychiatric disorders. *Mol. Psychiatry* **24**, 1248–1257 (2019).

88. K. Clancy, M. Ding, E. Bernat, N. B. Schmidt, W. Li, Restless 'rest': Intrinsic sensory hyperactivity and disinhibition in post-traumatic stress disorder. *Brain* **140**, 2041–2050 (2017).

89. K. J. Clancy, Q. Devignes, B. Ren, Y. Pollmann, S. R. Nielsen, K. Howell, P. Kumar, E. L. Belleau, I. M. Rosso, Spatiotemporal dynamics of hippocampal-cortical networks underlying the unique phenomenological properties of trauma-related intrusive memories. *Mol. Psychiatry* **29**, 2161–2169 (2024).

90. J. S. Stevens, R. Reddy, Y. J. Kim, S. J. H. van Rooij, T. D. Ely, S. Hamann, K. J. Ressler, T. Jovanovic, Episodic memory after trauma exposure: Medial temporal lobe function is positively related to re-experiencing and inversely related to negative affect symptoms. *Neuroimage Clin.* **17**, 650–658 (2018).

91. M. Kobelt, G. T. Waldhauser, A. Rupietta, R. Heinen, E. M. B. Rau, H. Kessler, N. Axmacher, The memory trace of an intrusive trauma-analog episode. *Curr. Biol.* **34**, 1657–1669.e5 (2024).

92. T. W. Schmitz, M. M. Correia, C. S. Ferreira, A. P. Prescot, M. C. Anderson, Hippocampal GABA enables inhibitory control over unwanted thoughts. *Nat. Commun.* **8**, 1311 (2017).

93. M. C. Anderson, J. G. Bunce, H. Barbas, Prefrontal-hippocampal pathways underlying inhibitory control over memory. *Neurobiol. Learn. Mem.* **134**, 145–161 (2016).

94. C. E. Flores, P. Méndez, Shaping inhibition: Activity dependent structural plasticity of GABAergic synapses. *Front. Cell. Neurosci.* **8**, 327 (2014).

95. C. Anacker, V. M. Luna, G. S. Stevens, A. Millette, R. Shores, J. C. Jimenez, B. Chen, R. Hen, Hippocampal neurogenesis confers stress resilience by inhibiting the ventral dentate gyrus. *Nature* **559**, 98–102 (2018).

96. P. W. Kalivas, M. P. Paulus, Eds., *Intrusive Thinking: From Molecules to Free Will* (The MIT Press, 2020).

97. S. Braem, J. M. Bugg, J. R. Schmidt, M. J. C. Crump, D. H. Weissman, W. Notebaert, T. Egner, Measuring adaptive control in conflict tasks. *Trends Cogn. Sci.* **23**, 769–783 (2019).

98. A. Putica, K. L. Felmingham, M. I. Garrido, M. L. O'Donnell, N. T. Van Dam, A predictive coding account of value-based learning in PTSD: Implications for precision treatments. *Neurosci. Biobehav. Rev.* **138**, 104704 (2022).

99. C. Teufel, P. C. Fletcher, Forms of prediction in the nervous system. *Nat. Rev. Neurosci.* **21**, 231–242 (2020).

100. T. Kube, M. Berg, B. Kleim, P. Herzog, Rethinking post-traumatic stress disorder – A predictive processing perspective. *Neurosci. Biobehav. Rev.* **113**, 448–460 (2020).

101. J. C. Hulbert, M. C. Anderson, What doesn't kill you makes you stronger: Psychological trauma and its relationship to enhanced memory control. *J. Exp. Psychol. Gen.* **147**, 1931–1949 (2018).

102. Y. Guo, T. W. Schmitz, M. Mur, C. S. Ferreira, M. C. Anderson, A supramodal role of the basal ganglia in memory and motor inhibition: Meta-analytic evidence. *Neuropsychologia* **108**, 117–134 (2018).

103. L. Schwabe, K. Nader, J. C. Pruessner, Reconsolidation of human memory: Brain mechanisms and clinical relevance. *Biol. Psychiatry* **76**, 274–280 (2014).

104. V. J. H. Ritvo, N. B. Turk-Browne, K. A. Norman, Nonmonotonic plasticity: How memory retrieval drives learning. *Trends Cogn. Sci.* **23**, 726–742 (2019).

105. H. C. Barron, T. P. Vogels, T. E. Behrens, M. Ramaswami, "Inhibitory engrams in perception and memory" in *Proceedings of the National Academy of Sciences* (PNAS, 2017), p. 201701812.

106. T. J. Ryan, P. W. Frankland, Forgetting as a form of adaptive engram cell plasticity. *Nat. Rev. Neurosci.* **23**, 173–186 (2022).

107. American Psychiatric Association, *Diagnostic and Statistical Manual of Mental Disorders* (American Psychiatric Association, ed. 5, 2013); https://psychiatryonline.org/doi/book/10.1176/appi.books.9780890425596.

108. C. Zlotnick, C. L. Franklin, M. Zimmerman, Does "subthreshold" posttraumatic stress disorder have any clinical relevance? *Compr. Psychiatry* **43**, 413–419 (2002).

109. A. Syssau, N. Font, Évaluations des caractéristiques émotionnelles d'un corpus de 604 mots. *Bull. Psychol.* , 361–367 (2005).

110. M. B. Brodeur, E. Dionne-Dostie, T. Montreuil, M. Lepage, The bank of standardized stimuli (BOSS) a new set of 480 normative photos of objects to be used as visual stimuli in cognitive research. *PLOS ONE* **5**, e10773 (2010).

111. T. D. Wager, T. E. Nichols, Optimization of experimental design in fMRI: A general framework using a genetic algorithm. *Neuroimage* **18**, 293–309 (2003).

112. J. Daunizeau, H. E. M. den Ouden, M. Pessiglione, S. J. Kiebel, K. E. Stephan, K. J. Friston, Observing the observer (I): Meta-bayesian models of learning and decision-making. *PLOS ONE* **5**, e15554 (2010).

113. R. A. Rescorla, A. R. Wagner, "A theory of Pavlovian conditioning: Variations in the effectiveness of reinforcement" in *Classical Conditioning II: Current Research and Theory* (Appleton-Century-Crofts, 1972), pp. 64–69.

114. R. E. Kalman, A new approach to linear filtering and prediction problems. *J. Basic Eng.* **82**, 35–45 (1960).

115. P. Dayan, S. Kakade, P. R. Montague, Learning and selective attention. *Nat. Neurosci.* **3**, 1218–1223 (2000).

116. C. Mathys, J. Daunizeau, K. J. Friston, K. E. Stephan, A bayesian foundation for individual learning under uncertainty. *Front. Hum. Neurosci.* **5**, 39 (2011).

117. K. J. Friston, L. Harrison, W. Penny, Dynamic causal modelling. *Neuroimage* **19**, 1273–1302 (2003).

118. R. G. Benoit, M. C. Anderson, Opposing mechanisms support the voluntary forgetting of unwanted memories. *Neuron* **76**, 450–460 (2012).

119. L. Fan, H. Li, J. Zhuo, Y. Zhang, J. Wang, L. Chen, Z. Yang, C. Chu, S. Xie, A. R. Laird, P. T. Fox, S. B. Eickhoff, C. Yu, T. Jiang, The human Brainnetome Atlas: A new brain atlas based on connectional architecture. *Cereb. Cortex* **26**, 3508–3526 (2016).

120. W. D. Penny, K. E. Stephan, J. Daunizeau, M. J. Rosa, K. J. Friston, T. M. Schofield, A. P. Leff, Comparing families of dynamic causal models. *PLOS Comput. Biol.* **6**, e1000709 (2010).

121. L. Rigoux, K. E. Stephan, K. J. Friston, J. Daunizeau, Bayesian model selection for group studies — Revisited. *Neuroimage* **84**, 971–985 (2014).

122. P. A. Yushkevich, J. B. Pluta, H. Wang, L. Xie, S.-L. Ding, E. C. Gertje, L. Mancuso, D. Kliot, S. R. Das, D. A. Wolk, Automated volumetry and regional thickness analysis of hippocampal subfields and medial temporal cortical structures in mild cognitive impairment. *Hum. Brain Mapp.* **36**, 258–287 (2015).

123. L. E. M. Wisse, H. J. Kuijf, A. M. Honingh, H. Wang, J. B. Pluta, S. R. Das, D. A. Wolk, J. J. M. Zwanenburg, P. A. Yushkevich, M. I. Geerlings, Automated hippocampal subfield segmentation at 7T MRI. *AJNR Am. J. Neuroradiol.* **37**, 1050–1057 (2016).

124. P. Berens, CircStat: A MATLAB toolbox for circular statistics. *J. Stat. Softw.* **31**, 1–21 (2009).

125. K. A. Grisanzio, A. N. Goldstein-Piekarski, M. Y. Wang, A. P. Rashed Ahmed, Z. Samara, L. M. Williams, Transdiagnostic Symptom Clusters and Associations With Brain, Behavior, and Daily Function in Mood, Anxiety, and Trauma Disorders. *JAMA Psychiatry* **75**, 201–209 (2018). https://doi.org/10.1001/jamapsychiatry.2017.3951.